# Erythroid overproduction of erythroferrone causes iron overload and developmental abnormalities in mice

Richard Coffey[1], Grace Jung[1], Renata C. Pereira[3], Elizabeta Nemeth[1] and Tomas Ganz[1, 2]

Departments of Medicine[1], Pathology[2] and Pediatrics[3], David Geffen School of Medicine at UCLA

Los Angeles, California 90095, USA

Corresponding Author: Tomas Ganz, PhD, MD

E-mail: tganz@mednet.ucla.edu

**Summary**

Erythroferrone, a glycoprotein hormone produced by erythroid cells in response to hemorrhage, hypoxia or other erythropoietic stimuli, suppresses the hepatic production of the iron-regulatory hormone hepcidin and thereby mobilizes iron for erythropoiesis. Erythroferrone is thought to interfere with paracrine BMP signaling that regulates hepcidin transcription in hepatocytes. Erythroferrone is pathologically overproduced in anemias with ineffective erythropoiesis but its contribution to the clinical manifestations of these anemias is not well understood. We generated three lines of transgenic mice with graded erythroid overexpression of erythroferrone and showed that they developed dose-dependent iron overload, impaired hepatic BMP signaling and relative hepcidin deficiency. At the highest levels of erythroferrone overexpression the mice manifested decreased perinatal survival, impaired growth, small hypofunctional kidneys, decreased gonadal fat depots and neurobehavioral abnormalities, all consistent with impaired organ-specific BMP signaling during development. Neutralizing excessive erythroferrone in congenital anemias with ineffective erythropoiesis may not only prevent iron overload but may have additional benefits for growth and development.

## Introduction

Systemic iron homeostasis is tightly regulated by the hepatic hormone hepcidin, which is secreted into blood plasma and inhibits intestinal iron absorption and the mobilization of stored iron (Nemeth et al., 2004). Erythropoietic activity is highly dependent on an adequate iron supply and is a strong regulator of iron homeostasis. During physiological response to anemia, renal hypoxia increases erythropoietin (EPO) production to stimulate the formation and differentiation of erythroid precursors. Within hours after EPO induction, hepcidin is suppressed (Liu et al., 2012) increasing iron flows into blood plasma and iron delivery to the marrow to support the enhanced production of erythrocytes. In anemias with ineffective erythropoiesis, in which EPO levels are increased and the erythropoietic compartment is disproportionately expanded, hepcidin is pathologically suppressed (Jones et al., 2015; Kearney et al., 2007) resulting in excessive iron absorption and eventual iron overload, even when the patients do not receive blood transfusions. The suppression of hepcidin in any condition with increased erythropoietic activity, and especially in anemia with ineffective erythropoiesis, is attributable to erythroid-derived factors (Pak et al., 2006). Search for such factors led to the discovery of erythroferrone (ERFE), a hormone produced by erythroblasts that acts on the liver to suppress hepcidin expression by hepatocytes (Kautz et al., 2014b).

Recent evidence indicates that ERFE inhibits hepcidin expression by antagonizing select members of the bone morphogenetic protein (BMP) family (Arezes et al., 2018; Wang et al., 2020). BMP signaling in hepatocytes regulates hepcidin transcription in response to plasma iron concentrations and hepatic iron stores, and the pathological loss of BMP signaling causes hepcidin deficiency and systemic iron overload (Canali et al., 2017; Koch et al., 2017). Specifically, BMP2 and 6 secreted by the sinusoidal endothelial cells in the liver are the key regulators of hepcidin transcription (Wang et al., 2020). ERFE lowers hepcidin transcription by sequestering the BMP2/6 heterodimer (Wang et al., 2020), but ERFE was also reported to bind other BMPs including BMP2, 4, 5, 6 and 7 (Arezes et al., 2020a; Arezes et al., 2018). Considering that BMP signaling has pleiotropic effects beyond its role in iron homeostasis, the endocrine effects of ERFE may not be limited to hepcidin regulation in the liver. BMP signaling is involved in the regulation of development and homeostasis in multiple organs, including the kidney, vestibular system of the inner ear, and skeletal system. Deletion of *Bmp7* in mice leads to severely impaired kidney development (Dudley et al., 1995; Luo et al., 1995), resulting in renal insufficiency, and the administration of exogenous BMP7 in a rat model of kidney fibrosis protects against damage and restores function in damaged kidneys (Morrissey et al., 2002). Deficiency of BMP4 results in impaired vestibular function and hearing loss (Blauwkamp et al., 2007). Appropriate BMP signaling is also required for normal bone and growth plate development. Mice overexpressing BMP antagonists develop osteopenia, resulting in bone fractures (Devlin et al., 2003b; Gazzerro et al., 2005), and genetic deletion of BMP receptors leads to impaired growth plate development (Yoon et al., 2005).

Although substantial evidence supports the role of ERFE as a stress hormone that acutely suppresses hepatic hepcidin synthesis in response to erythropoietic stimuli, much less is known about the chronic effects of ERFE *in vivo*. The effect of chronically elevated ERFE levels have been analyzed in the context of erythropoietic disorders such as β-thalassemia (Ganz et al., 2017). However, while patients with β-thalassemia commonly suffer from problems that could be linked to disruptions in BMP signaling, including iron overload (Papakonstantinou et al., 2009), renal impairment (Musallam and Taher, 2012), and skeletal problems such as impaired growth (Rodda et al., 1995) or bone mineralization (Karimi et al., 2007), it is unclear to which extent the observed pathologies are attributable to elevated ERFE as opposed to other factors such as tissue and organ hypoxia, the effects of hemolytic products or the toxicity of treatment. To increase ERFE production, animal models rely on anemia (Kautz et al., 2015; Kautz et al., 2014a) or erythropoietin (EPO) administration (Coffey et al., 2018) but serum ERFE levels measured in these models are orders of magnitude lower than in human patients with β-thalassemia (Ganz et al., 2017). Additionally, high EPO levels exert multiple systemic effects (Suresh et al., 2019) beyond increasing *Erfe* expression and these complicate direct attribution of observed phenotypes to the action of ERFE alone .

The aim of the current study was to determine the effect of chronically elevated *Erfe* expression on systemic iron homeostasis and BMP signaling, independent of the effects of chronic anemia or EPO treatment and at a range of circulating ERFE levels similar to those present in humans with β-thalassemia and other anemias with

ineffective erythropoiesis. To this end we have generated multiple lines of novel transgenic mice overexpressing graded levels of erythroferrone in erythroid cells. We find that chronically elevated *Erfe* expression results in dose-dependent hepcidin suppression, dysregulation of iron homeostasis and tissue iron accumulation. Additionally, at high levels, chronic *Erfe* overexpression affects multiple organ systems influencing pup survival, kidney function, and behavior.

## Materials and Methods

### Animal husbandry and experiments

A DNA construct previously used to target gene overexpression to cells of the erythroid lineage under control of the human locus control region (µLCR) and β-globin gene promoter was generously contributed by Dr. Kenneth R. Peterson (Peterson et al., 2004) and adapted to express N-FLAG-*mErfe*. Transgenic founder animals were generated at Cyagen labs by pronuclear injection of fertilized C57BL/6N zygotes. One transgenic founder generated by this method gave rise to the high-expressing "H" line as well as produced the founder of the moderately expressing "M" line, and the second transgenic founder, generated by pronuclear injection, gave rise to the low-expressing "L" line. Individual transgenic lines were established and experimental mice generated by breeding heterozygous transgenic mice with C57BL/6J mice to yield transgenic mice and wild-type littermate controls. Each mouse was genotyped to ensure stability of transgene copy number. Animals were fed a natural ingredient diet (Labdiet 5053) containing ~220 ppm iron and housed in a specific-pathogen-free barrier facility. Animal body weights were recorded weekly beginning at 3 weeks and until euthanasia, either at 6 or 16 weeks of age. Experimental animals were euthanized by isoflurane inhalation. All experiments involving mice were conducted with the approval of the University of California, Los Angeles Animal Research Committee.

### Genomic characterization

Genomic DNA was prepared from the livers of the H-line transgenic founder, H-line F1 progeny, M-line founder, and one M-line F1 progeny using Qiagen Gentra Purgene kit per manufacturer's instructions. Genomic sequencing on paired-end libraries was performed at UCLA Technology Center for Genomics & Bioinformatics using an Illumina Novaseq S4 DNA sequencer. The reads were aligned to the reference genomic sequence Mus musculus strain C57BL/6J chromosome 4, GRCm38.p6 C57BL/6J and to the transgene sequence, and overlap sequences between adjacent transgene copies and between transgene and chromosomal sequence identified and used to ascertain the chromosomal insertion site, and transgene copy number.

### Measurement of iron-related and hematological parameters

Serum iron and liver non-heme iron were measured by using a colorimetric assay according to the manufacturer's protocol (Sekisui Diagnostics). Prior to sampling, livers were homogenized to reduce variation resulting from regional differences in hepatic iron deposition. Hemoglobin levels, red-blood-cell counts, and hematocrit % were determined by using a HemaVet blood analyzed (Drew Scientific).

### Quantification of serum and urinary proteins and metabolites

Serum ERFE concentrations were determined as previously described (Kautz et al., 2015) with the substitution of DELFIA europium-conjugated streptavidin for horseradish peroxidase conjugated streptavidin. Fluorescence was measured by CLARIOstar plate reader. Serum hepcidin concentrations were determined by ELISA as detailed previously (Kautz et al., 2014b). Serum urea nitrogen concentrations were measured by using the QuantiChrom Urea Assay Kit (BioAssay Systems), urinary albumin using the Mouse Albumin ELISA Kit (Abcam, ab108792) and urinary creatinine using the Creatinine (urinary) Colorimetric Assay Kit (Cayman Chemical), all in accordance with the manufacturers' protocols.

### RNA isolation and measurement of gene expression

Total RNA isolation was performed by using TRIzol (ThermoFisher Scientfic). cDNA was synthesized using the iScript cDNA Sythesis Kit (Bio-Rad) following the manufacturer's protocol. Relative mRNA expression for genes of interest were determined by quantitative RT-PCR using SsoAdvanced Universal SYBR Green Supermix (Bio-

Rad) and measured on a CFX-96 RT-PCR Detection System (Bio-Rad). Primer sequences used in this study are listed in Supplemental Table 1.

*Behavioral testing*

All behavioral testing was performed at the UCLA behavioral testing core facility by personnel blinded to the mouse genotype. Mice were transferred to the testing facility and allowed 1 week to acclimate prior to testing between 11 and 13 weeks of age. Open-field testing was performed for a duration of 30 minutes in an empty and dimly lit, light intensity less than 20 lux, square area measuring 30 cm per side. Mouse movement was recorded automatically and analyzed by using ANY-maze software (Stoelting). Righting reflex of experimental animals was assessed by flipping animals held by the tail, so that the animal passed through an inverted position, to an approximate height of 25 cm. Landing position of the mouse was recorded and a score of 0, 1, or 2 given to mice that landed on their feet (0), side (1), or back (2), respectively. Righting reflex testing was performed three times per mouse and the highest value recorded. Negative geotaxis testing was assessed by placing mice facing downwards on a declined surface. Mouse movement was recorded for a duration of 30 s and a score of 0, 1, 2, or 3 was given to mice that turned to face upslope and climbed (0), turned without climbing (1), moved without turning (2), or did not move (3). Reaction to auditory stimulation was measured by the degree of visible response to a 20 KHz sound with a volume of 90 dB at mouse location. A score of 0, 1, 2, or 3 was given to mice that did not respond (0), exhibited a pinna reflex (1), jumped < 1 cm (2), or jumped > 1 cm (3). Wire maneuvering capacity was assessed by the ability of mice to hang onto a wire and navigate to an attachment post when allowed to initially establish a foreleg grip. A score of 0, 1, 2, 3, or 4 was assigned to mice that demonstrated active hindleg grip (0), impaired hindleg grip (1), inability to grip with hindlegs (2), inability to lift legs followed by falling (3), or immediately falling (4).

*Bone histomorphometry analysis*

Mouse femurs were dehydrated and fixed in 70% ethanol prior to embedding in methyl methacrylate. Sections cut longitudinally at a thickness of 5 μm were stained with toluidine blue (pH 6.4) and used for static bone parameter analysis on a total of 20 fields per sample by using a OsteoMeasure morphometry system (Osteometics, Atlanta) at a distance of 200 μm from the growth plate. Results for individual parameters are listed using accepted units and terminology recommended by the Histomorphometry Nomenclature Committee of the American Society for Bone and Mineral Research (Dempster et al., 2013).

*Statistical analysis*

Statistical analysis was performed by using the statistical package included in Prism version 8 (GraphPad). $P<0.05$ was considered statistically significant. For each individual transgenic mouse line and its wild-type littermates, means of experimental groups, defined by genotype and sex, were compared with others by using either student's *t*-test, Welch's ANOVA, or Two-way ANOVA where indicated. In the event of significant differences between group means after one-way ANOVA analysis, individual group means were compared by using an unpaired-*t*-test with Welch's correction. Significant interaction between variables during two-way ANOVA testing was followed by Šidak's multiple comparisons test to determine significant differences between wild-type and transgenic mice within each sex. Analysis of observed vs expected ratios when analyzing transgene inheritance was performed by using binomial testing and an expected transgene incidence of 50%. Fisher's exact test was used to analyze differences in phenotypic incidence between groups. In behavioral analysis, to identify outliers in a group of mice, ROUT analysis (Prism version 8, GraphPad) was performed with a false discovery rate set at 0.1%.

## Results

*Generation of Erfe-overexpressing mice*

To model the erythroid overexpression of *Erfe* in anemias with ineffective erythropoiesis (Kautz et al., 2014b), we targeted transgenic *Erfe* expression to erythroid cells. We generated mice that selectively overexpress *Erfe* in erythroid cells by pronuclear injection with a transgene construct that placed *Erfe* expression under the control of the human β-globin promoter and the β-globin locus control region **(Figure 1A)**. Transgenic mice from all lines
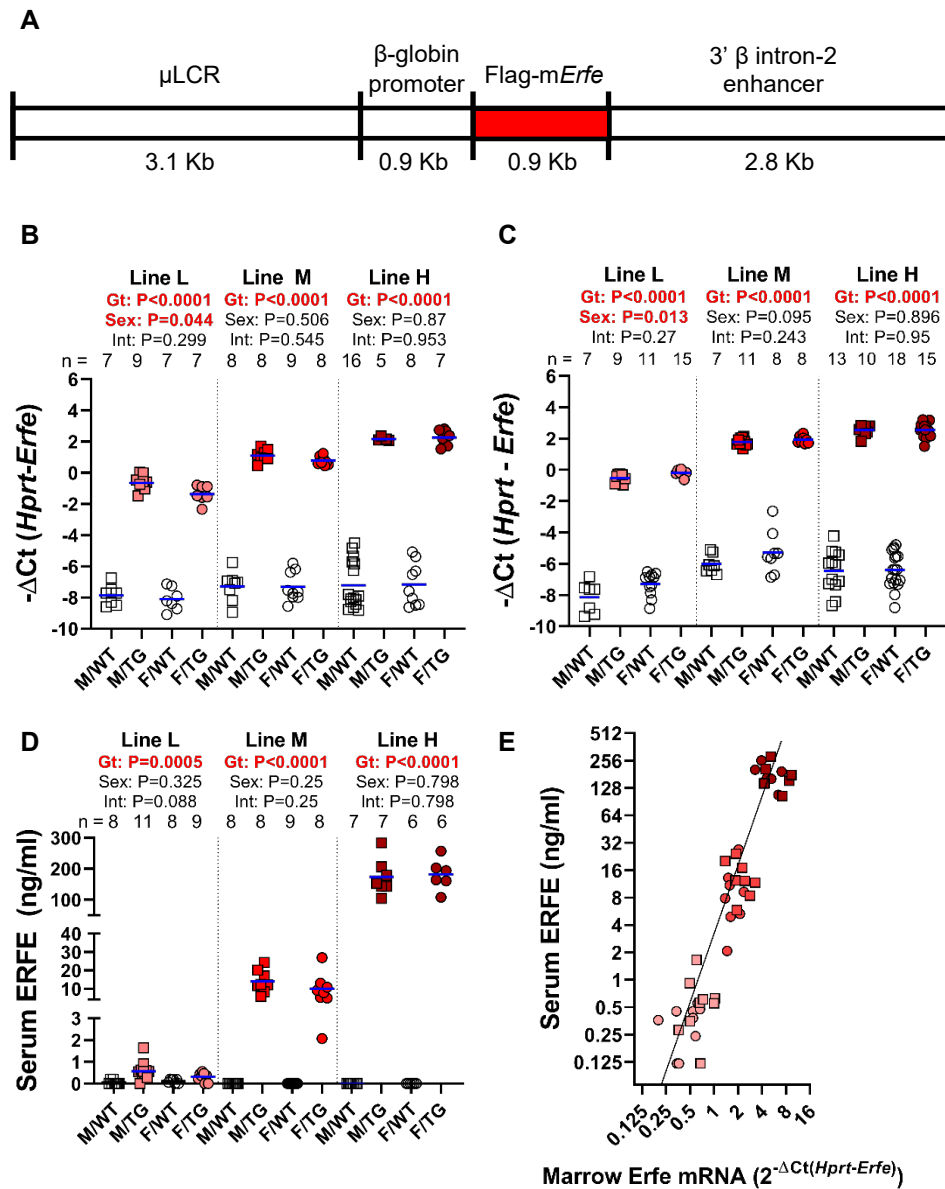
**Figure 1. Generation of Hbb-*Erfe* mice and analysis of *Erfe* overexpression. A)** Structure of the transgene construct. Bone marrow *Erfe* mRNA in **B**) 6 week-old and **C**) 16-week old mice. **D)** Serum ERFE levels of 6-week-old mice, **E)** Relationship between serum ERFE protein levels and marrow *Erfe* mRNA, regression line $Y=3.19 * X^{2.5}$ ($r^2 = 0.51$). In all panels, male (M, square) and female (F, round); mean of each group is shown by blue line, TG = *Erfe*-overexpressing mice (line-L pink, line-M red, and line-H dark red symbols) and WT = wild-type littermate controls (white symbols). Within each individual transgenic line, groups were compared by two-way ANOVA to determine significant effects ($P<0.05$, bold red) of genotype and sex on data variation and to identify interactions between these variables. Cohort numbers for mRNA and serum analysis are shown.

had elevated bone marrow *Erfe* expression relative to wild-type littermate controls **(Figure 1B)**. Bone marrow *Erfe* mRNA expression differed between the three lines leading us to identify the respective lines as high (line-H), medium (line-M), and low (line-L) *Erfe*-overexpressing mice. Lines H and M had been derived from the highest-expressing founder. Genomic sequencing identified the haploid transgene insertion site on Chr. 4, from 11985998 to 12010497, overlapping into gene 1700123M08Rik noncoding RNA of unknown function. The H and M lines differed by transgene copy number (3 vs 1), resulting from a rare spontaneous deletion of two tandem copies of the transgene. Line-L was derived from another lower-expressing founder and was not further genomically characterized. Transgene expression was similar at 6- and 16-week time points chosen for detailed analysis **(Figure 1B, C)**.

Serum ERFE levels in line-L transgenic mice were near the threshold of detection by ELISA, below levels measured in WT mice after EPO injection or in Hbb[Th3/+] thalassemic mice (Kautz et al., 2015). Compared with

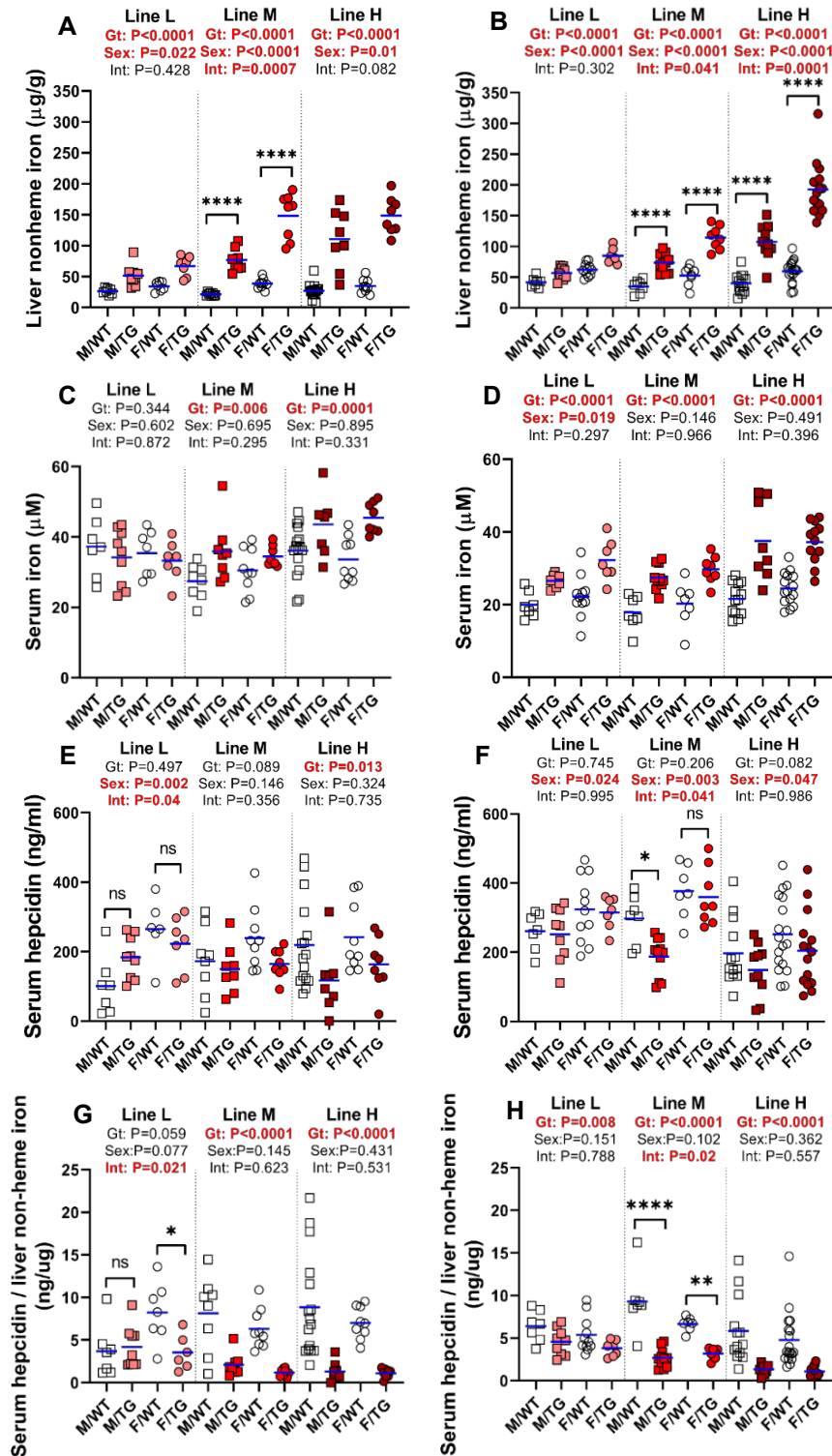line-L, serum ERFE levels were 20x higher in line-M and 200x in line-H transgenic mice **(Figure 1D).**



**Figure 2.** *Erfe* **overexpression causes dose-dependent iron accumulation and inadequate hepcidin expression.** Liver non-heme iron (**A, B**), serum iron (**C, D**), serum hepcidin (**E, F**), and serum hepcidin relative to liver iron (**G, H**) levels at 6 (**A, C, E, G**) and 16 (**B, D, F, H**) weeks of age in male (M) and female (F) *Erfe*-overexpressing (TG) mice and wild-type (WT) littermate controls from line-L (white/pink), line-M white/red), and line-H (white/dark red). ); mean of each group is shown in blue. For each mouse line, groups were compared by two-way ANOVA to determine effects of genotype and sex on data variation (significant differences denoted in bold red) and to identify interactions between these variables. In the event of significant interaction between genotype and sex, individual groups were compared by Šidak's multiple comparisons test (ns=P$\geq$0.05, *=P<0.05, **=P<0.01, ***=P<0.001, ****=P<0.0001).
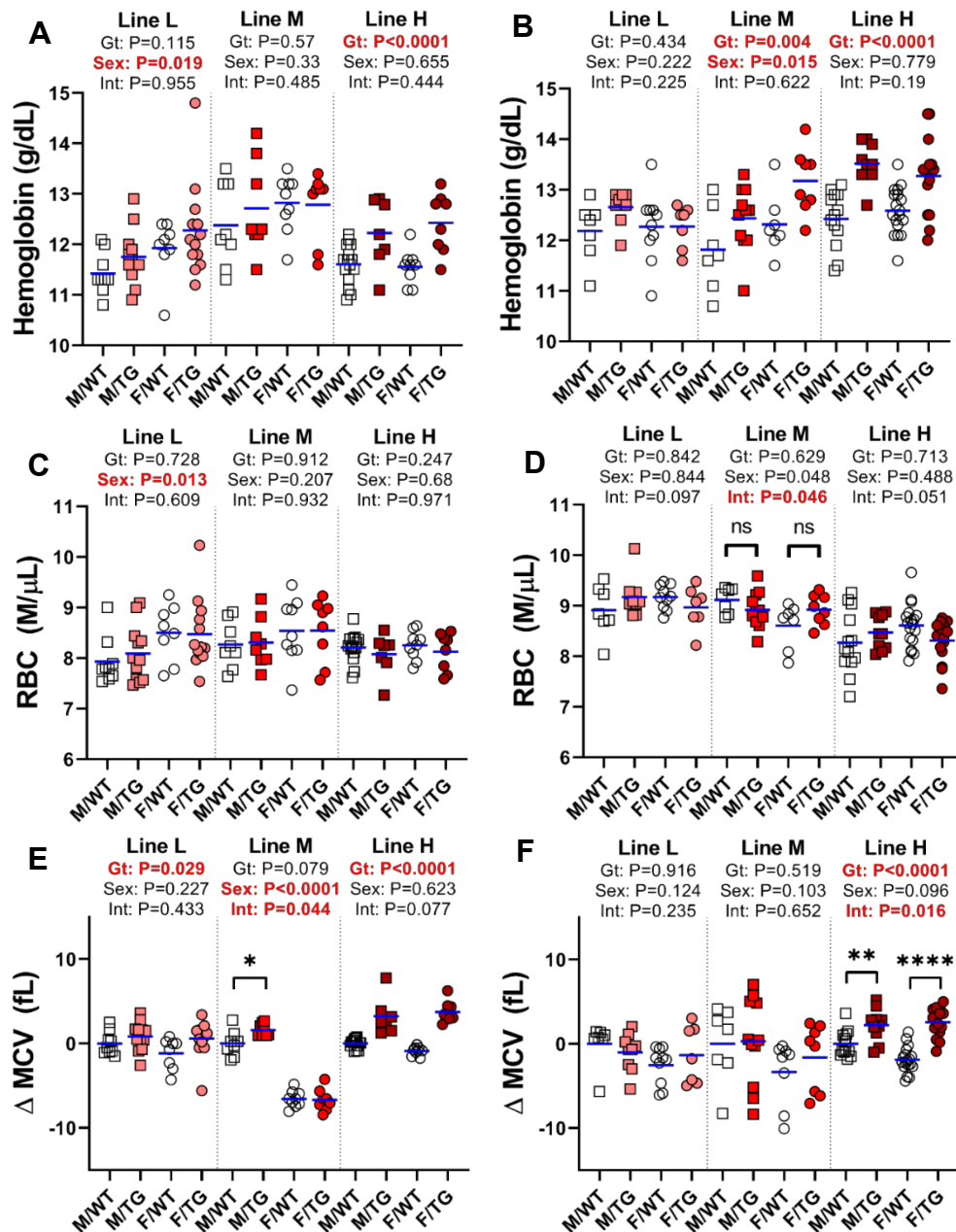
**Figure 3: ERFE enhances erythropoiesis in a dose-dependent manner.** Hemoglobin levels (**A**, **B**), red blood cell (RBC) counts (**C, D**), and differences in MCV relative to male wild-type (WT) littermates (**E**, **F)** at 6 (**A, C, E**) and 16 (**B, D, F**) weeks of age in male (M) and female (F) *Erfe*-overexpressing (TG) mice and WT littermate controls from line-L (white/pink), line-M (white/red), and line-H (white/dark red), ); mean of each group is shown in blue. Groups within each individual line were compared by two-way ANOVA to determine significant effects of genotype and sex on data variation and to identify interactions between these variables (P<0.05 denoted in bold red). In the event of significant interaction between genotype and sex, individual groups were compared by Šidak's multiple comparisons test (NS=P≥0.05, *=P<0.05, **=P<0.01, ***=P<0.001, ****=P<0.0001).

Interestingly, moderate differences in mRNA bone marrow *Erfe* expression led to much larger differences in circulating ERFE levels between transgenic lines **(Figure 1E)**.

*Erfe overexpression causes iron overload and elevated hemoglobin levels*

*Erfe* overexpression increased liver non-heme iron levels in a dose-dependent fashion. At 6 weeks of age, transgenic mice from lines L, M and H respectively loaded ~2, ~3.6 and ~4.2 times more liver non-heme iron than their wild-type littermate controls **(Figure 2A)**. The effect of elevated *Erfe* expression on liver iron accumulation persisted in 16-week-old transgenic mice **(Figure 2B)**. In all transgenic lines at both ages, females

had higher liver iron levels than males, consistent with the previously described sex differences in iron loading of the C57BL/6 strain (Courselaud et al., 2004). Serum iron was also elevated in both male and female transgenic mice from line-M and H, but not line-L, at 6 weeks of age **(Figure 2C),** and elevated in transgenic mice aged 16 weeks in all lines relative to wild-type littermates **(Figure 2D)**.

Serum hepcidin concentrations in *Erfe*-transgenic mice would be expected to be determined by the balance between the suppressive effect of ERFE on hepcidin synthesis and the stimulatory effect of increased hepatic and plasma iron concentrations (Corradini et al., 2011; Ramos et al., 2011).  In line-L transgenic mice at 6 or 16 weeks of age, serum hepcidin concentrations were similar to those of WT mice **(Figure 2E, F)**, consistent with these transgenic mice reaching a stable level of iron overload by 6 weeks. In line M, the mean serum hepcidin concentrations were lower in transgenic than WT mice but this reached statistical significance only in males at 16 weeks. In line-H, hepcidin was significantly suppressed in both sexes at 6 weeks.  Importantly, the ratio of serum hepcidin concentrations to liver non-heme iron content indicates inappropriately low hepcidin production relative to the severity of iron loading in all transgenic groups except for 6-week old, line-L males. **(Figure 2G, H)**.

At both 6 and 16 weeks of age, transgenic mice from line-H had elevated hemoglobin levels **(Figure 3A, B)** but not RBC counts **(Figure 3C, D)**. Increased hemoglobin levels were attributable to larger erythrocytes **(Figure 3E, F).** We did not detect consistent differences in hematological parameters between transgenic and wild-type mice in the M or L line.

*Tissue-selective effect of Erfe overexpression on BMP signaling*

ERFE has recently been reported to act as a BMP antagonist (Arezes et al., 2020a; Arezes et al., 2018). The high concentration of erythroid *Erfe*-overexpressing cells in the bone marrow raised the possibility that ERFE may locally suppress BMP signaling in that organ. However, we found no suppressive effect of ERFE on the expression of the BMP target genes *Smad7* or *Id1* at 6 weeks of age **(Figure S1A-B),** and *Bmp2* or *Bmp6* expression in the bone marrow was also not affected **(Figure S1C-D).**

To determine if chronic *Erfe* overexpression in erythroid cells impairs BMP signaling in the liver, an organ which suppresses hepcidin in response to acute increases in ERFE levels within the physiologic range, we measured the expression of the BMP-responsive genes *Hamp, Smad7 and Id1* in livers from *Erfe*-overexpressing mice and wild-type littermates at 6 weeks of age. At higher *Erfe* expression levels, we detected a suppressive effect on the hepatic expression *Hamp* and *Smad7* but not *Id1* **(Figure 4A-C)**.  We also assessed the effect of ERFE on the expression of BMP ligands, specifically *Bmp2* and *Bmp6* that play critical roles in iron sensing by the liver (Canali et al., 2017; Koch et al., 2017). There was no effect of *Erfe* overexpression on the hepatic mRNA levels of *Bmp2* and *Bmp6* **(Figure 4D-E)**.

*Erfe overexpression affects growth and organ size*

ERFE circulates in blood and its effects on BMP signaling could therefore affect morphogenesis and homeostasis in any organ or tissue. We detected a dose-dependent effect of ERFE on body weight, with higher levels of ERFE resulting in lower body weights. Male transgenic mice from line-H had consistently reduced body weights, compared with wild-type littermates, between the ages of 3 and 16 weeks **(Figure 5A).** Female transgenic mice from Line-H also maintained lower body weights after weaning but the difference between female transgenic and wild-type mice resolved with age. A small but significant effect of genotype on body weight was also detected in transgenic mice from line-M, with male transgenic mice displaying a larger difference from wild-type controls compared to female transgenic mice **(Figure S2A)**. Transgenic mice from line-L, of either sex, did not differ in weight compared with wild-type littermates **(Figure S3A)**. Analysis of selected tissues and organs revealed a reduction in the size of gonadal fat pads and kidneys, even after adjusting for reduced total body weight, in line-H transgenic mice at 6 and 16 weeks of age **(Figure 5B, C).** Smaller kidney size in line-H transgenic mice was associated with reduced kidney function as indicated by elevated serum urea nitrogen levels at 6 and 16 weeks of age **(Figure 5D)**. However, kidney morphology did not appear altered as a result of *Erfe* overexpression in this line and we detected no increase in proteinuria, as determined by urinary albumin to creatinine ratio, in line-H transgenic mice compared with wild-type littermates at 16 weeks of age **(Figure 5E)**.
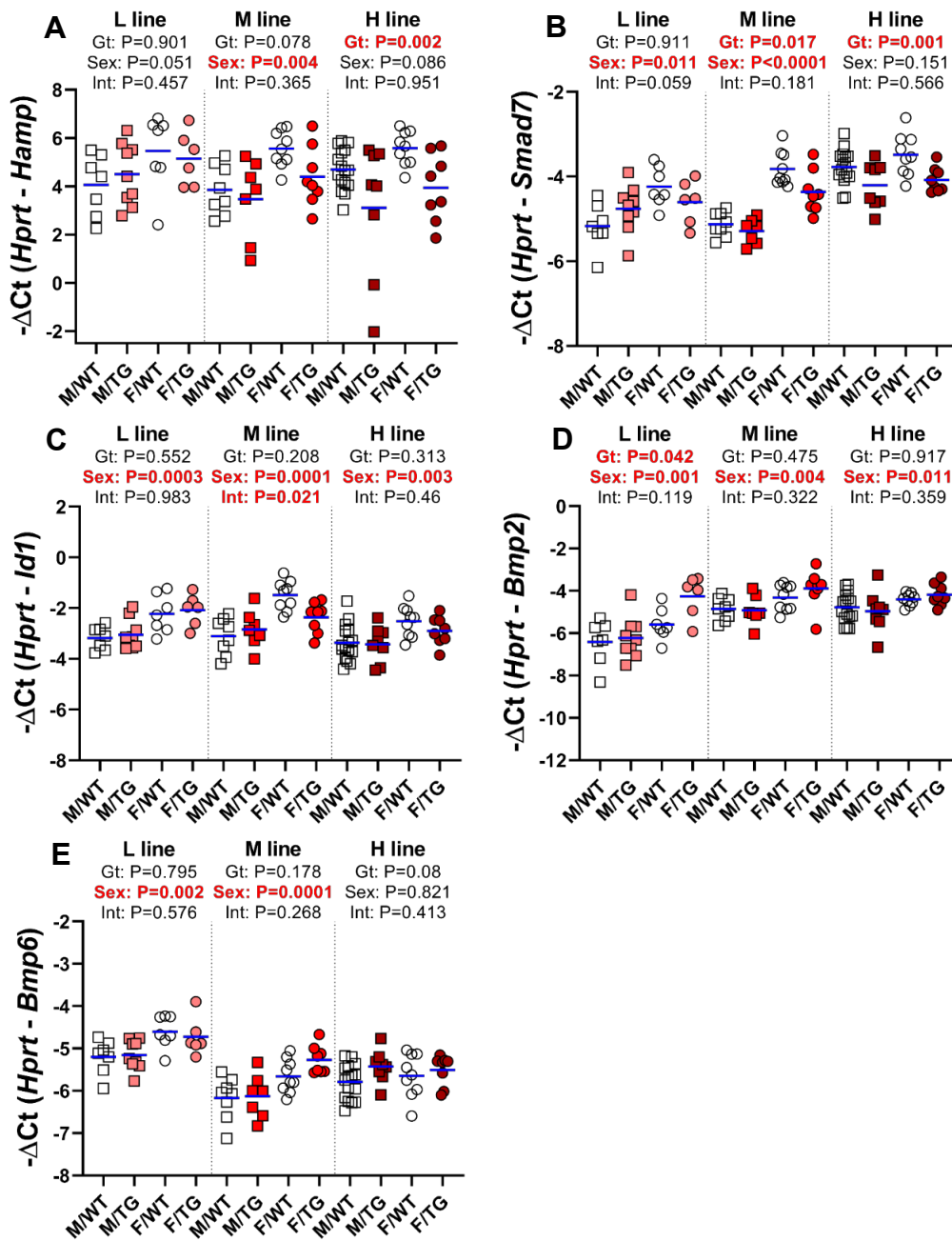
**Figure 4. Effect of *Erfe* overexpression on liver BMP signaling.** Relative mRNA expression of **A)** *Hamp*, **B)** *Smad7*, **C)** *Id1*, **D)** *Bmp2* and **E)** *Bmp6* in the liver at 6 weeks of age in male (M) and female (F) *Erfe*-overexpressing (TG) mice and wild-type (WT) littermate controls from line-L (white/pink), line-M (white/red), and line-H (white/dark red), mean of each group is shown in blue. Groups within each individual line were compared by two-way ANOVA to determine significant effects of genotype and sex on data variation and to identify interactions between these variables (P<0.05 denoted in bold red). In the event of significant interaction between genotype and sex, individual groups were compared by Sidak's multiple comparisons test (NS=P≥0.05, *=P<0.05, **=P<0.01, ***=P<0.001, ****=P<0.0001).

In line-M no differences in individual tissue weights were detected with the exception of lower relative kidney size in line-M transgenic mice compared with wild-type littermates that was statistically significant in females, at 16 weeks of age **(Figure S2B-I)**. No effect of *Erfe* overexpression on individual tissue or organ weights was detected in line-L mice **(Figure S3B-E)**. Among other tissues analyzed from line-H mice **(Figure S4)**, the only consistent difference in weight, present at both 6 and 16 weeks of age, between transgenic mice and wild-type controls was the brain. Brain weights from transgenic mice comprised a greater relative proportion of total body weight compared with those of wild-type littermates **(Figure S4A)**. However, this difference was primarily attributable to

the lower body weights of transgenic mice rather than an absolute difference in brain weights, which were the same in transgenic and wild-type littermates. *Erfe* overexpression resulted in significantly reduced inguinal white adipose tissue in 6-week-old, line-H transgenic mice **(Figure S4B)** and elevated spleen weights **(Figure S4E)**, relative to total body weights, but these differences were not observed at 16 weeks of age.



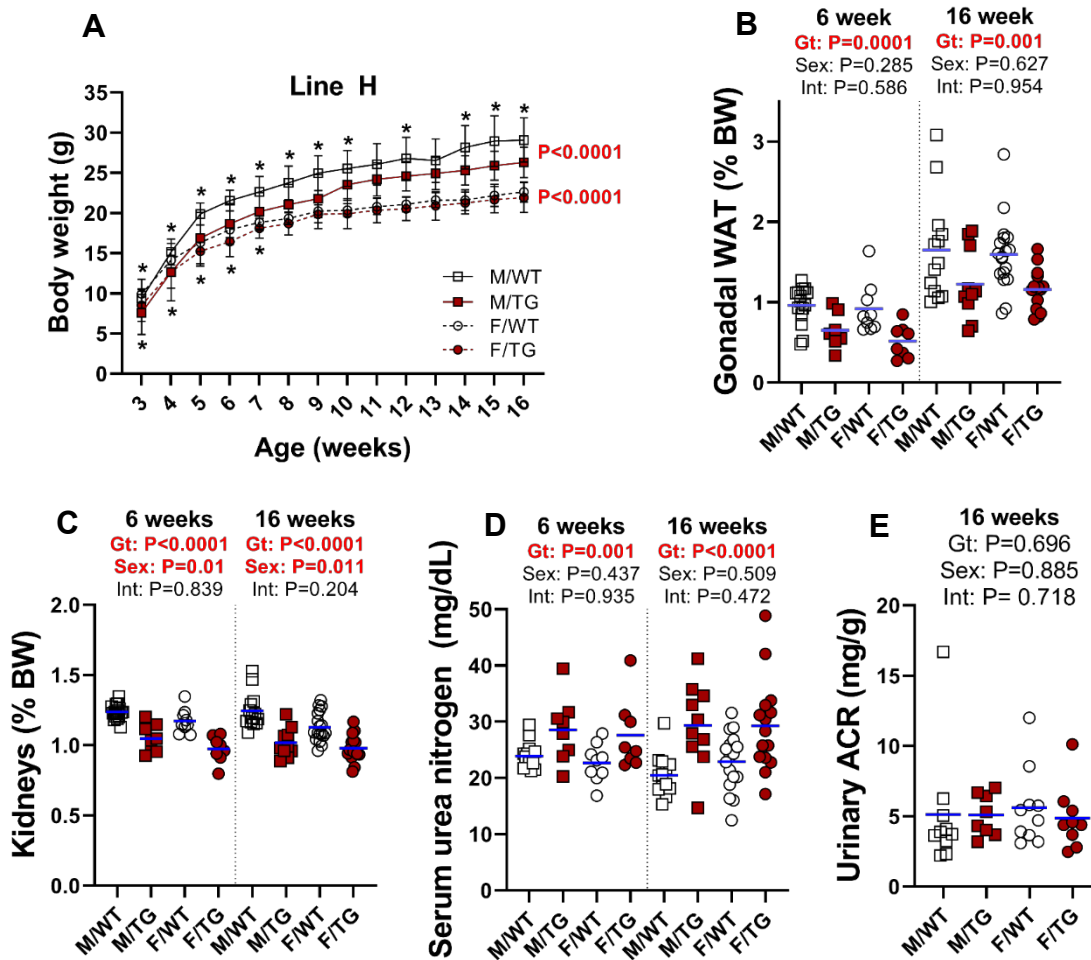**Figure 5. High ERFE expression causes reduced body and kidney mass in line-H mice. A)** Growth curves from ages 3 to 16 weeks of age. Statistical significance of the effect of genotype on data variation between body weights of sex-matched wild type (WT) and transgenic (TG) mice determined by 2-way ANOVA are displayed to the right of their respective curves. Statistically significant differences (P<0.05) between sex-matched WT and TG body weights at individual time points, determined by Student's *t*-test, are indicated by asterisks (*) above or below curves for males and females, respectively. **B)** Decreased mass of gonadal white adipose tissue (WAT) pads and **C)** kidneys from line-H mice as a percentage of total body weight at 6 and 16 weeks of age. **D)** Serum blood urea nitrogen (BUN) in line-H mice at 6 and 16 weeks of age and **E)** urinary albumin-creatinine ratio (ACR) in line-H mice at 16 weeks of age. Groups at each age were compared by two-way ANOVA to determine significant effects of genotype and sex on data variation and to identify interactions between these variables (P<0.05 denoted in bold red). In the event of significant interaction between genotype and sex, individual groups were compared by Šidak's multiple comparisons test (NS=P≥0.05, *=P<0.05, **=P<0.01, ***=P<0.001, ****=P<0.0001).

As bone development and homeostasis is regulated by BMP signaling (Bandyopadhyay et al., 2006; Mishina et al., 2004; Tsuji et al., 2006), we performed bone histomorphometry in female line-H mice at 6 weeks of age to analyze the effect of erythroid overexpression of *Erfe* on steady-state bone homeostasis. We detected no significant differences in any measured parameters of bone development, mineralization, or cell populations **(Table S2)**. Although *Erfe*-overexpressing mice tended to have increased osteoid thickness relative to wild-type littermates this difference was not statistically significant.
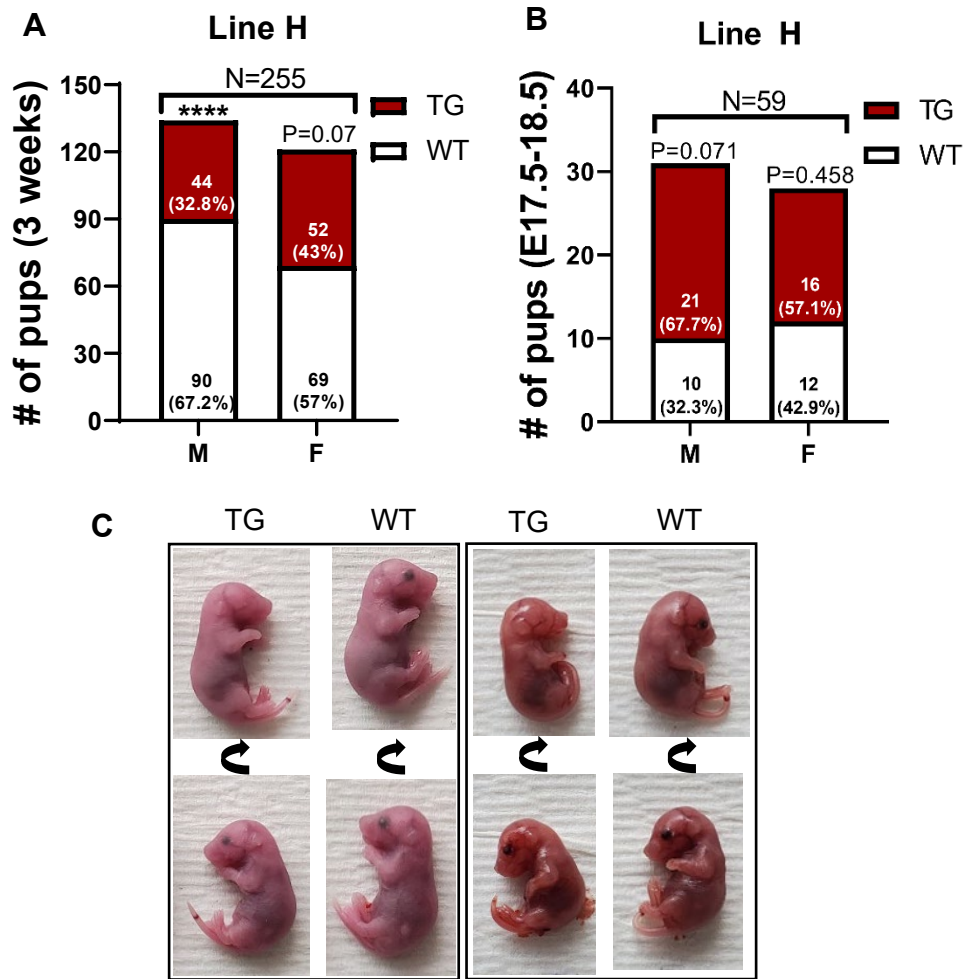
**Figure 6. Impaired postnatal survival and unilateral anophthalmia in line-H transgenic mice.** Number and within-sex percentage of wild-type (WT) and transgenic (TG) mice, grouped by sex, from line-H breeding surviving at **A)** 3 weeks of age or **B**) in utero at embryonic day 17.5-18.5. Statistically significant differences from expected proportions were assessed by binomial testing. **C**) Examples of unilateral anophthalmia in line-H TG mice. Top and bottom panels show the same pup rotated to demonstrate, in TG mice, normal (bottom) or impaired (top) eye development compared with WT littermates.

*Erfe overexpression impairs pup survival and causes developmental and behavioral abnormalities*

In line-H mice, we detected divergence from the predicted mendelian ratio of 50% transgenic pups generated by breeding monoallelic transgenic mice with wild-type mice. The percentage of transgenic mice from line-H surviving to weaning was lower than in their WT littermates. Males were more severely affected with only 32.8 % of surviving pups being transgenic compared with 43% in females **(Figure 6A)**. This difference in inheritance was highly statistically significant for males and borderline significant for females. Reduced survival of male transgenic pups was observed regardless of dam genotype. To determine if this divergence from expected mendelian inheritance was attributable to loss of pups during embryonic development, we analyzed genotypes from line-H pups towards the end of gestation between embryonic day 17.5 and 18.5. Here the proportion of transgenic to wild-type pups did not significantly differ from the expected ratio of 50%, and there was a nonsignificant trend towards a greater than expected proportion of male mice being transgenic (**Figure 6B**).

Together these data suggest a postnatal loss of male transgenic mice from line-H. No divergence from expected transgene inheritance ratios was observed in litters from either line-L or line-M breeding (**Figure S5).** Line-H transgenic mice also occasionally presented with permanent eyelid closure of a single eye, occurring in approximately 5% of transgenic mice from this line. Unilateral anophthalmia was seen in developing embryos between days E17.5 and 18.5 in approximately 5% of transgenic mice but not in wild-type littermates **(Figure 6C)**. Eye abnormalities were not observed in transgenic mice from either line-M or line-L.

11

Transgenic mice from line-H displayed compulsive circling behavior detectable as early as 3 weeks of age and the behavior persisted with aging **(Supplemental video file).** Circling had incomplete penetrance, affecting 38% of line-H transgenic mice with similar incidence in males and females, but was not observed in wild-type littermates **(Figure 7A)**. Compulsive circling was not observed in transgenic mice from either line-M or L.
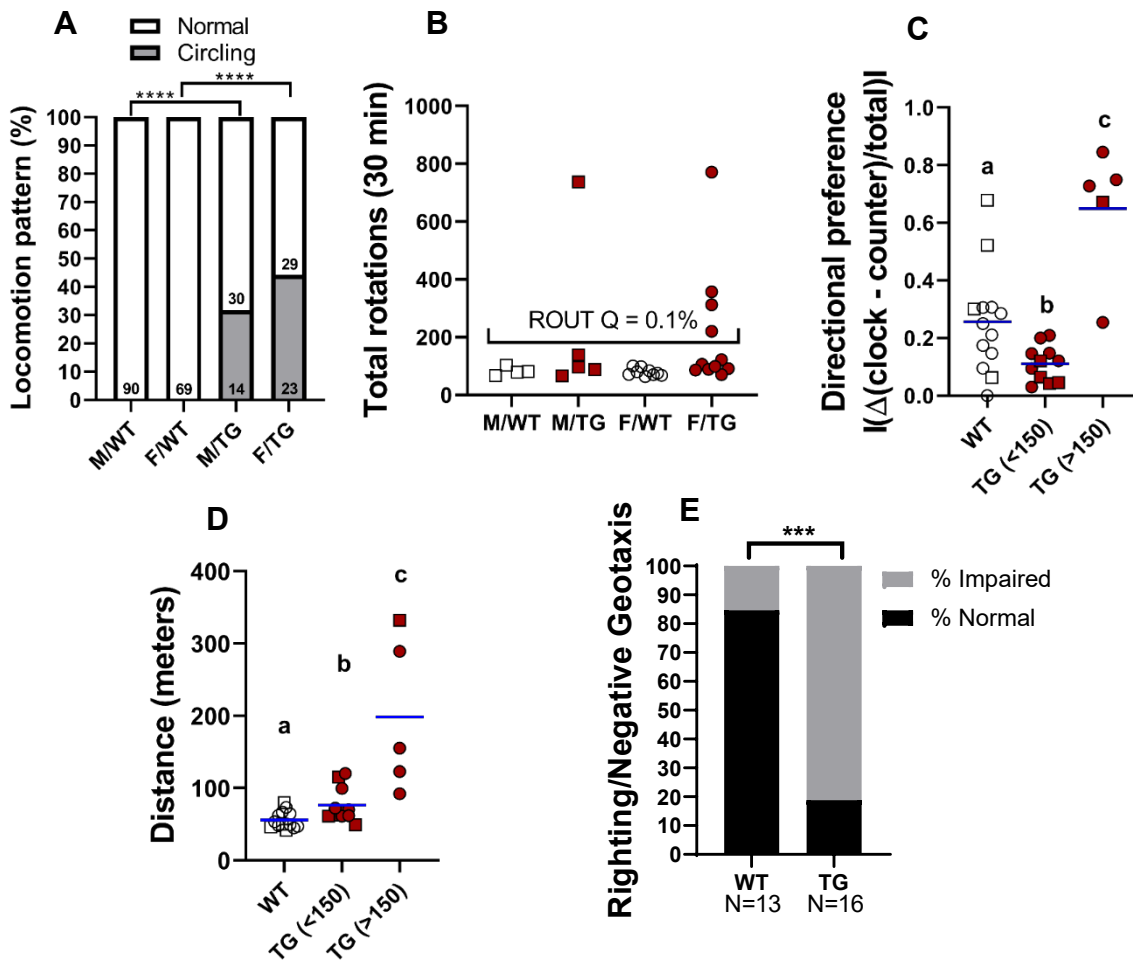


**Figure 7. Repetitive circling behavior and impaired motor/vestibular function in line-H transgenic mice. A)** Incidence of overt circling behavior in line-H mice. Numerical values on bars indicate animal number per pattern of movement. Statistically significant differences in locomotion pattern between groups of the same sex were determined by Fisher's exact test (****=P<0.0001). **B)** Total rotations completed by mice during open-field testing. Groups were pooled and analyzed for outliers by ROUT test at false discovery rate Q=0.1%. P<0.05 by Fisher exact test for proportion of outliers in TG vs WT mice. **C)** Absolute values of rotation-direction preference and **D)** total distance traveled by line-H mice during open-field testing. Groups of WT mice, TG mice with fewer than 150 rotations during testing (TG (<150)), and TG mice with greater than 150 rotations during testing (TG (>150)) were compared by one-way ANOVA and groups not sharing a common letter superscript are significantly different (P<0.05). **E)** Incidence of impaired outcomes during righting reflex or negative geotaxis testing in line-H mice. A mouse was designated as "impaired" if its combined score from the righting reflex and negative geotaxis testing was >0. Mice categorized as normal had a combined score of 0 on these tests. Statistical significance of the difference in incidence of impairment between groups was determined by Fisher's exact test (***P<0.001).

To detect any associated neurobehavioral abnormalities, we performed a battery of behavioral tests in line-H mice between 11 and 13 weeks of age. During a 30 minute open field test, using automated measurement of mouse movement, mice previously identified as displaying the circling phenotype manifested a greatly increased number of rotations while the majority of transgenic mice exhibited a similar number of rotations as their wild-type littermates **(Figure 7B)**. Data from male and female mice were combined as analysis by two-way ANOVA indicated no effect of sex on parameters measured during open field testing **(Figure S6)**. By ROUT outlier analysis **(Figure 7B)**, transgenic mice were considered high-circling if they performed more than 150 rotations during open field testing, ~1.5x the highest number of rotations observed in wild-type mice. Individual high-

circling transgenic mice displayed a clear preference for a single direction of rotation **(Figure 7C)**, but as a group had no overall preference for either the clockwise or counter-clockwise direction **(Figure S6A)**. The direction of rotation in individual mice was random in low-circling transgenic mice **(Figure 7C)**. During the open field test high-circling transgenic mice were more active and traveled a greater distance compared with low-circling transgenic mice and wild-type littermates **(Figure 7D)**. A significant difference in activity between wild-type and low-circling transgenic mice was also detected, attributable to several low-circling transgenic mice that exhibited a greater amount of rotations during testing than any recorded in wild-type mice but failed to reach the predetermined threshold to be included in the high-circling group.

To determine if the observed circling phenotype was associated with alterations in vestibular-motor function, we tested the righting reflex and the negative geotaxis response in line-H mice. Transgenic mice from this line demonstrated righting-reflex impairment and a trend towards an impaired negative geotaxis response compared with wild-type littermates **(Figure S6C, D)**. As both these tests measure spatial orientation and neuromuscular coordination, and as mice that exhibited impairment in either of these test did not necessarily exhibit impairment in both tests, we combined the results of these tests into a binary categorization of mice as either performing on these respective tests without detected problems or displaying impairment. Compared with wild-type littermates a significantly higher percentage of line-H transgenic mice displayed impairment in either righting or negative geotaxis **(Figure 7E)**, suggesting that high *Erfe* overexpression is associated with altered vestibular-motor function. *Erfe*-overexpressing and wild-type mice were equally responsive to auditory stimulation and demonstrated similar physical capacity during a wire maneuver test.

## Discussion

Extensive evidence supports that erythroid-derived ERFE acts on the liver to suppress hepcidin expression in response to acute erythropoietic stimuli (Kautz et al., 2014b). ERFE may also contribute to iron overload in disorders with chronic ineffective erythropoiesis, as suggested by normalization of hepcidin expression by ablation of *Erfe* in a murine Th3/+ model of β-thalassemia (Kautz et al., 2015). However, the complex effects of anemia, tissue hypoxia and hemolysis in this model complicate any direct attribution of phenotypic features in thalassemia to the effects of ERFE alone. In this study we report that constant, high-level *Erfe* expression by erythroid cells is sufficient by itself to attenuate hepcidin responsiveness to iron loading, and to cause systemic iron overload manifested by increased plasma iron concentrations and hepatic tissue iron stores. The characterization of multiple transgenic mouse lines expressing varying levels of *Erfe* allowed for the investigation of the effect of graded ERFE concentrations on systemic iron homeostasis. Serum ERFE levels in the three lines of transgenic mice characterized in this study ranged from ~0.5 ng/ml, similar to levels we measured contemporaneously in Hbb$^{th3/+}$ mice, to ~200 ng/ml, on par with the highest levels reported in humans with β-thalassemia (Ganz et al., 2017). This wide range of serum ERFE concentrations far exceeded the difference in expression at the mRNA level between these lines, ~8x between line-L and H, and suggests decreasing clearance of plasma ERFE at high concentrations. Analysis of liver iron content between transgenic lines indicates that the effect of erythron-derived ERFE on iron loading is both dose-dependent and saturable at high levels, as liver iron loading only moderately increased between line-L, -M, and -H transgenic mice, despite substantially higher serum ERFE levels. Additionally, liver iron accumulation observed in *Erfe*-overexpressing mice in this study was generally milder than in Hbb$^{th3/+}$ mice, suggesting iron overload in β-thalassemia is not solely attributable to the chronic increase in *Erfe* expression. This conclusion is consistent with previous reports of incomplete correction of iron overload in Hbb$^{th3/+}$ mice that lacked ERFE or received treatment with inhibitory anti-ERFE antibodies (Arezes et al., 2020b; Kautz et al., 2015).

Liver hepcidin expression is feedback-regulated by liver iron content and serum iron concentrations (Arezes et al., 2020a; Ramos et al., 2011). Any suppression of hepcidin by ERFE will cause increased duodenal iron absorption and hepatic iron accumulation, which in turn raises hepcidin concentrations and inhibits iron absorption, eventually reaching concentrations of hepcidin that maintain a steady state in which iron accumulation balances iron losses. Iron loading in *Erfe*-overexpressing mice of the same line changed little between 6 and 16 weeks of age in this study, indicating that by the age of 6 weeks enough iron accumulated to

raise hepcidin to the point of iron balance. Our serum hepcidin measurements in *Erfe*-overexpressing mice support this concept as at 6 weeks of age only line-H *Erfe*-overexpressing mice had significantly suppressed serum hepcidin levels and in all groups of transgenic mice, with the exception of line-M males, serum hepcidin concentrations were normalized by 16 weeks of age. The delay in establishment of the iron/hepcidin balance in line-H transgenic mice is indicative of the dose-dependent nature of this process as higher circulating levels of ERFE require greater accumulation of iron to stimulate hepcidin expression sufficiently to overcome the effects of ERFE. The hepcidin levels in *Erfe*-overexpressing mice in iron balance are similar to those of wild-type littermates but are inadequate when considered in the context of serum and hepatic iron concentrations.

We observed that line-H *Erfe*-overexpressing mice had consistently elevated blood hemoglobin concentrations but not increased erythrocyte numbers, indicative of higher erythrocyte hemoglobin content when compared with wild-type littermates. *Erfe*-overexpressing mice from line-M had elevated hemoglobin concentrations at 16 weeks but not at 6 weeks when their somatic and erythron growth rates were faster. The consistency of these effects across ages in line-H mice, compared with those from line-M, may be attributable to more profound hepcidin suppression and subsequent iron availability in this line, compared with line-L or -M mice, as erythropoiesis in mice and humans is modestly enhanced by hepcidin suppression and increased iron availability (Hanudel et al., 2017; McCranor et al., 2013). Unlike in mice with physiological erythropoiesis, in the mouse model of β-thalassemia hepcidin suppression and increased iron supply <u>worsen</u> ineffective erythropoiesis and anemia, as shown by improved hemoglobin concentrations after interventions that increase hepcidin (Casu et al., 2016; Gardenghi et al., 2010). A recent report of the detrimental effects of a genetic *Erfe* variant that increased ERFE production in congenital dyserythropoietic anemia type II supports the possibility that chronically elevated ERFE production and the resulting excess of iron may also worsen anemia in human disorders of ineffective erythropoiesis (Andolfo et al., 2019).

We examined our model for evidence that the observed effects of ERFE were mediated by suppression of BMP signaling. Although specifics of the interaction between ERFE and individual BMPs may vary by species (Melchert et al., 2020), ERFE is reported to interact with BMP2, 4, 5, 6, 7, and a heterodimer of BMP2/6 (Arezes et al., 2020a; Arezes et al., 2018; Wang et al., 2020). To determine if *Erfe* overexpression alters BMP signaling in vivo we assessed the expression of the BMP-responsive genes *Id1* (Korchynskyi and ten Dijke, 2002) and *Smad7* (Mleczko-Sanecka et al., 2010) in the liver, a peripheral tissue responsive to ERFE, as well as the bone marrow, a population of cells that could be subject to the autocrine or paracrine effects of erythroid-derived ERFE. In the liver we identified a suppressive effect of moderate or high *Erfe* overexpression on *Smad7*, but not *Id1* expression. Despite the potential for local BMP inhibition by erythroid *Erfe* overexpression, we did not detect a decrease in the expression of *Id1* or *Smad7* in the bone marrow of *Erfe*-overexpressing mice compared with wild-type littermates. This lack of effect is unlikely to be attributable to a compensating increase in BMP expression by cells in the marrow as expression of *Bmp2* and *Bmp6* did not show a dose-dependent trend towards increased expression across lines of *Erfe*-overexpressing mice. Differential sensitivity of tissues to the effects of ERFE suggests that the mechanism of ERFE action may depend on differences in local BMP signaling mechanisms. The sensitivity of certain cell types over others to the action of ERFE raises the possibility of an alternative, receptor-based mechanism of ERFE signaling in addition to acting as a BMP antagonist. However, no receptor for ERFE has yet been identified, despite unbiased screens by our lab and others.

While the abnormalities in transgenic mice with low to moderate circulating levels of ERFE were almost entirely limited to iron homeostasis, line-H transgenic mice displayed a multifaceted phenotype including increased postnatal mortality, reduced body weight and gonadal adipose tissue weight, reduced kidney size and function, occasional unilateral anophthalmia, and compulsive circling behavior. We considered the possibility that the multiple abnormalities in line-H were caused by disruption of a critical gene at the site of transgene insertion. However, we found no evidence for this possibility by genomic sequencing. Specifically, lines-M and -H, derived from the same founder but differing in transgene copy number, share the same insertion site on Chr. 4 overlapping a gene for a noncoding RNA of unknown function and the corresponding genomic sequence on the other copy of Chr. 4 is wild-type. Rather, the spectrum of abnormalities in line-H transgenic mice is consistent with disruption of signaling by select BMPs during embryonic development or early growth. BMP signaling plays a key role in a wide range of physiological processes involved in both the development and homeostatic

14

maintenance of various organs (Bandyopadhyay et al., 2006; Blauwkamp et al., 2007; Dudley et al., 1995; Yoon et al., 2005). ERFE was also identified as a vascular morphogen in Xenopus embryos where it acts by antagonizing BMP4 (Melchert et al., 2020). Our observations raise the possibility that some of the nonhematologic complications experienced by patients with ineffective erythropoiesis (Karimi et al., 2007; Musallam and Taher, 2012; Rodda et al., 1995) could either be caused or exacerbated by disrupted BMP signaling.

Deletion of *Bmp7* in mice leads to impaired embryonic kidney development (Karsenty et al., 1996; Luo et al., 1995). In the present study line-H transgenic mice kidney size was reduced compared to wild-type littermates and this manifested as reduced kidney function without evidence of kidney malformation or disruption of the barriers that prevent protein loss in urine. We also detected an effect on eye development in line-H mice, with a small percentage of *Erfe*-overexpressing mice presenting with unilateral anophthalmia. Eye development is regulated, in part, by BMP signaling (Dudley et al., 1995; Karsenty et al., 1996) and disruption of BMP signaling by conditional deletion of BMP receptors in the eye during embryonic development leads to anophthalmia (Murali et al., 2005). In the present study we did not observe any instances of bilateral anophthalmia and in eyes that successfully developed we detected no morphological differences. The observed abnormalities in kidney size and eye development in line-H, *Erfe*-overexpressing mice may result from altered BMP signaling in utero as transgene expression controlled by the construct used to generate *Erfe*-overexpressing mice in this study is reported to occur in erythroid cells at early stages of embryonic development as well as postnatal life (Peterson et al., 2004). BMP signaling is also linked to the development of the vestibular system of the inner ear in mice (Blauwkamp et al., 2007), potentially providing an explanation for the compulsive circling behavior seen in a subset of line-H transgenic mice. Behavioral testing revealed that while less than half of line-H transgenic mice exhibit obvious circling behavior, most display some degree of vestibular-motor dysfunction, as determined by either an altered righting reflex or response during negative geotaxis testing. BMP4 is required for normal vestibular function and BMP4$^{+/-}$ mice demonstrate circling behavior (Blauwkamp et al., 2007), similar to line-H transgenic mice in the present study. While mouse ERFE is reported to not inhibit BMP4 (Melchert et al., 2020), ERFE may interact with and inhibit BMP4 heterodimers formed with other BMPs, e.g. BMP7 (Kim et al., 2019).

We found that body weight and postnatal survival were also affected by high-level *Erfe* overexpression. *Erfe*-overexpressing mice from line-H had lower body weights during early life, prior to weaning, but both sexes demonstrated either a similar or increased rate of growth after weaning, suggesting that the observed difference in body weight early in life may be due to problems with suckling that begin to resolve with the adoption of solid food. Altered postnatal survival and decreased body weights were more prominent in male line-H *Erfe*-overexpressing mice compared with females, despite similar circulating ERFE levels between sexes. This difference in phenotype severity based on sex may be attributable to differences in basal, tissue-specific expression of BMPs between sexes, with female mice expressing greater levels of BMPs, driven by estrogen signaling (Ong et al., 2004; Zhou et al., 2003), possibly compensating for BMP inhibition by ERFE. In this study we detected a significant effect of sex on liver *Bmp2* and *Bmp6* expression with higher-relative expression in females compared with males across all transgenic lines, with the exception of *Bmp6* expression in Line-H. However, in the bone marrow we did not find a consistent effect of sex on *Bmp2* or *Bmp6* expression across mouse lines, suggesting that the sex-related differences in the liver may be the result of higher liver iron levels in female mice.

In line-H transgenic mice compared with wild-type littermates, we consistently observed a reduction in the relative mass of gonadal white adipose tissue, a visceral fat deposit. The mass of subcutaneous inguinal fat was also reduced in this line but only at 6 weeks of age. Adipogenesis is regulated by nuanced interplay between BMP signaling and antagonism (Blazquez-Medela et al., 2019) (Gustafson et al., 2015), suggesting that ERFE may modulate adipocyte homeostasis through BMP inhibition. A preferential effect of ERFE on visceral fat compared with subcutaneous fat, as the present study suggests, may be due to differences in the expression of, or receptivity to, specific BMPs by adipocytes or adipose progenitor cells in these compartments (Guiu-Jurado et al., 2016) (Macotela et al., 2012). ERFE is reported to alter BMP2 signaling in a "depot-specific" manner *in vitro*, altering BMP signaling to a greater degree in adipocytes derived from some adipose compartments compared

with others (Denton et al., 2019). Reduced adiposity in response to *Erfe* overexpression also supports previous findings of increased adipose deposit size in *Erfe*-deficient mice (Little et al., 2019).

A well-documented complication of β-thalassemia is a loss of bone mineral density associated with marrow expansion driven by chronic erythropoietic stimulation (Tyler et al., 2006). We hypothesized that high-level *Erfe* expression in nearby erythroid cells of the bone marrow would result in altered BMP signaling in osteoblasts or osteoclasts and lead to alterations in bone mineralization or morphology, potentially contributing to observed bone remodeling in response to persistent anemia. However, we observed no clear difference in steady-state bone histomorphometry between line-H *Erfe*-overexpressing mice and wild-type controls. The lack of effect of ERFE on bone development and mineralization was unexpected given the substantial effects, including spontaneous fractures, observed in bones of mice overexpressing other BMP antagonists (Devlin et al., 2003a; Gazzerro et al., 2005). However, in these studies BMP antagonists were overexpressed selectively in cells of the osteoblast lineage and likely exhibited autocrine inhibition of BMP signaling in osteoblasts, unlike in the present study where endocrine or paracrine BMP inhibition by ERFE predominated. We found no evidence that increased systemic ERFE levels substantially alter bone homeostasis in mice during basal conditions.

The observed adverse effect of excessive ERFE production on kidney function is potentially relevant for patients with β-thalassemia who suffer from renal complications. Kidney dysfunction in the context of β-thalassemia is incompletely understood but thought to result from a combination of iron-mediated damage, chronic anemia with renal hypoxia, and treatment with iron chelators that may damage the kidney (Demosthenous et al., 2019). Signaling by BMP7 is thought to protect against renal fibrosis (Zeisberg et al., 2003) and increased expression of BMP antagonists may predispose the kidney to tubular injury (Yanagita et al., 2006), exacerbating damage from excess iron or chelation therapy. In this scenario, reducing the amount or activity of ERFE in patients with β-thalassemia may represent a potential therapeutic option for preventing kidney damage. It remains to be determined which aspects of the phenotype observed in mice with high circulating ERFE levels in this study are the result of altered BMP signaling in utero versus during postnatal life. Relative to human β-thalassemia, transgenic mice in this study may be more susceptible to abnormal organ development because of species differences in the timing of increased *Erfe* expression during embryonic and postnatal development. In humans with β-thalassemia, anemia and ineffective erythropoiesis does not develop until after birth (Blobel et al., 2015) because of the protective effect of fetal hemoglobin, whereas transgene expression in our mouse model begins early during embryonic development (Peterson et al., 2004). Therefore, increased *Erfe* expression, resulting from anemia in patients with β-thalassemia, is not expected until the postnatal period, diminishing the potential effects on organ development. However, elevated ERFE levels in utero would be expected in patients with fetal anemias such as occur in α-thalassemia, pyruvate kinase deficiency, congenital dyserythropoietic anemia and other congenital anemias with ineffective erythropoiesis (Blobel et al., 2015). In particular, elevated ERFE could contribute to developmental abnormalities seen in patients with severe α-globin deficiency (Songdej et al., 2017).

In conclusion, chronically increased blood ERFE levels contribute to iron loading and, at high levels, alter the development or homeostasis of multiple organ systems. ERFE may be a suitable therapeutic target in anemias from ineffective erythropoiesis to reduce iron loading and possible organ dysfunction from ERFE-mediated inhibition of BMP signaling.

## Acknowledgments

## Author Contributions

RC designed and performed experiments, analyzed data, and wrote the manuscript. GJ performed experiments and assisted with data interpretation. RCP performed bone analyses and assisted with their interpretation. EN and TG conceived the project, designed experiments, analyzed data, and wrote the manuscript.

## Declaration of Interests

TG and EN are scientific co-founders of Intrinsic LifeSciences and Silarus Pharma. TG is a consultant for ADARx, Akebia, Pharmacosmos, Ionis, Gossamer Bio, Global Blood Therapeutics, American Regent, Disc Medicine, and Rockwell Scientific. EN is a consultant for Protagonist, Ionis and Disc Medicine. TG and EN are inventors on patents related to erythroferrone. RC, RCP and GJ declare no conflicts.

## References

Andolfo, I., Rosato, B.E., Marra, R., De Rosa, G., Manna, F., Gambale, A., Iolascon, A., and Russo, R. (2019). The BMP-SMAD pathway mediates the impaired hepatic iron metabolism associated with the ERFE-A260S variant. Am J Hematol *94*, 1227-1235.

Arezes, J., Foy, N., McHugh, K., Quinkert, D., Benard, S., Sawant, A., Frost, J.N., Armitage, A.E., Pasricha, S.R., Lim, P.J., et al. (2020a). Antibodies against the erythroferrone N-terminal domain prevent hepcidin suppression and ameliorate murine thalassemia. Blood *135*, 547-557.

Arezes, J., Foy, N., McHugh, K., Sawant, A., Quinkert, D., Terraube, V., Brinth, A., Tam, M., LaVallie, E.R., Taylor, S., et al. (2018). Erythroferrone inhibits the induction of hepcidin by BMP6. Blood *132*, 1473-1477.

Arezes, J., Foy, N.J., McHugh, K., Quinkert, D., Benard, S., Sawant, A., Frost, J.N., Armitage, A.E., Pasricha, S.R., Lim, P.J., et al. (2020b). Antibodies against the erythroferrone N-terminal domain prevent hepcidin suppression and ameliorate murine thalassemia. Blood.

Bandyopadhyay, A., Tsuji, K., Cox, K., Harfe, B.D., Rosen, V., and Tabin, C.J. (2006). Genetic analysis of the roles of BMP2, BMP4, and BMP7 in limb patterning and skeletogenesis. PLoS Genet *2*, e216.

Blauwkamp, M.N., Beyer, L.A., Kabara, L., Takemura, K., Buck, T., King, W.M., Dolan, D.F., Barald, K.F., Raphael, Y., and Koenig, R.J. (2007). The role of bone morphogenetic protein 4 in inner ear development and function. Hear Res *225*, 71-79.

Blazquez-Medela, A.M., Jumabay, M., Rajbhandari, P., Sallam, T., Guo, Y., Yao, J., Vergnes, L., Reue, K., Zhang, L., Yao, Y., et al. (2019). Noggin depletion in adipocytes promotes obesity in mice. Mol Metab *25*, 50-63.

Blobel, G.A., Bodine, D., Brand, M., Crispino, J., de Bruijn, M.F., Nathan, D., Papayannopoulou, T., Porcher, C., Strouboulis, J., Zon, L., et al. (2015). An international effort to cure a global health problem: A report on the 19th Hemoglobin Switching Conference. Exp Hematol *43*, 821-837.

Canali, S., Zumbrennen-Bullough, K.B., Core, A.B., Wang, C.Y., Nairz, M., Bouley, R., Swirski, F.K., and Babitt, J.L. (2017). Endothelial cells produce bone morphogenetic protein 6 required for iron homeostasis in mice. Blood *129*, 405-414.

Casu, C., Oikonomidou, P.R., Chen, H., Nandi, V., Ginzburg, Y., Prasad, P., Fleming, R.E., Shah, Y.M., Valore, E.V., Nemeth, E., et al. (2016). Minihepcidin peptides as disease modifiers in mice affected by beta-thalassemia and polycythemia vera. Blood *128*, 265-276.

Coffey, R., Sardo, U., Kautz, L., Gabayan, V., Nemeth, E., and Ganz, T. (2018). Erythroferrone is not required for the glucoregulatory and hematologic effects of chronic erythropoietin treatment in mice. Physiol Rep *6*, e13890.

Corradini, E., Meynard, D., Wu, Q., Chen, S., Ventura, P., Pietrangelo, A., and Babitt, J.L. (2011). Serum and liver iron differently regulate the bone morphogenetic protein 6 (BMP6)-SMAD signaling pathway in mice. Hepatology *54*, 273-284.

Courselaud, B., Troadec, M.B., Fruchon, S., Ilyin, G., Borot, N., Leroyer, P., Coppin, H., Brissot, P., Roth, M.P., and Loreal, O. (2004). Strain and gender modulate hepatic hepcidin 1 and 2 mRNA expression in mice. Blood Cells Mol Dis *32*, 283-289.

Demosthenous, C., Vlachaki, E., Apostolou, C., Eleftheriou, P., Kotsiafti, A., Vetsiou, E., Mandala, E., Perifanis, V., and Sarafidis, P. (2019). Beta-thalassemia: renal complications and mechanisms: a narrative review. Hematology *24*, 426-438.

Dempster, D.W., Compston, J.E., Drezner, M.K., Glorieux, F.H., Kanis, J.A., Malluche, H., Meunier, P.J., Ott, S.M., Recker, R.R., and Parfitt, A.M. (2013). Standardized nomenclature, symbols, and units for bone histomorphometry: a 2012 update of the report of the ASBMR Histomorphometry Nomenclature Committee. J Bone Miner Res *28*, 2-17.

Denton, N.F., Eghleilib, M., Al-Sharifi, S., Todorcevic, M., Neville, M.J., Loh, N., Drakesmith, A., Karpe, F., and Pinnick, K.E. (2019). Bone morphogenetic protein 2 is a depot-specific regulator of human adipogenesis. Int J Obes (Lond) *43*, 2458-2468.

Devlin, R.D., Du, Z., Pereira, R.C., Kimble, R.B., Economides, A.N., Jorgetti, V., and Canalis, E. (2003a). Skeletal Overexpression of Noggin Results in Osteopenia and Reduced Bone Formation. Endocrinology *144*, 1972-1978.

Devlin, R.D., Du, Z., Pereira, R.C., Kimble, R.B., Economides, A.N., Jorgetti, V., and Canalis, E. (2003b). Skeletal overexpression of noggin results in osteopenia and reduced bone formation. Endocrinology *144*, 1972-1978.

Dudley, A.T., Lyons, K.M., and Robertson, E.J. (1995). A requirement for bone morphogenetic protein-7 during development of the mammalian kidney and eye. Genes Dev *9*, 2795-2807.

Ganz, T., Jung, G., Naeim, A., Ginzburg, Y., Pakbaz, Z., Walter, P.B., Kautz, L., and Nemeth, E. (2017). Immunoassay for human serum erythroferrone. Blood *130*, 1243-1246.

Gardenghi, S., Ramos, P., Marongiu, M.F., Melchiori, L., Breda, L., Guy, E., Muirhead, K., Rao, N., Roy, C.N., Andrews, N.C., et al. (2010). Hepcidin as a therapeutic tool to limit iron overload and improve anemia in beta-thalassemic mice. J Clin Invest *120*, 4466-4477.

Gazzerro, E., Pereira, R.C., Jorgetti, V., Olson, S., Economides, A.N., and Canalis, E. (2005). Skeletal overexpression of gremlin impairs bone formation and causes osteopenia. Endocrinology *146*, 655-665.

Guiu-Jurado, E., Unthan, M., Bohler, N., Kern, M., Landgraf, K., Dietrich, A., Schleinitz, D., Ruschke, K., Kloting, N., Fasshauer, M., et al. (2016). Bone morphogenetic protein 2 (BMP2) may contribute to partition of energy storage into visceral and subcutaneous fat depots. Obesity (Silver Spring) *24*, 2092-2100.

Gustafson, B., Hammarstedt, A., Hedjazifar, S., Hoffmann, J.M., Svensson, P.A., Grimsby, J., Rondinone, C., and Smith, U. (2015). BMP4 and BMP Antagonists Regulate Human White and Beige Adipogenesis. Diabetes *64*, 1670-1681.

Hanudel, M.R., Rappaport, M., Gabayan, V., Jung, G., Salusky, I.B., Nemeth, E., Ganz, T., and Zaritsky, J. (2017). Increased serum hepcidin contributes to the anemia of chronic kidney disease in a murine model. Haematologica *102*, e85-e88.

Jones, E., Pasricha, S.R., Allen, A., Evans, P., Fisher, C.A., Wray, K., Premawardhena, A., Bandara, D., Perera, A., Webster, C., et al. (2015). Hepcidin is suppressed by erythropoiesis in hemoglobin E beta-thalassemia and beta-thalassemia trait. Blood *125*, 873-880.

Karimi, M., Ghiam, A.F., Hashemi, A., Alinejad, S., Soweid, M., and Kashef, S. (2007). Bone mineral density in beta-thalassemia major and intermedia. Indian Pediatr *44*, 29-32.

Karsenty, G., Luo, G., Hofmann, C., and Bradley, A. (1996). BMP 7 is required for nephrogenesis, eye development, and skeletal patterning. Ann N Y Acad Sci *785*, 98-107.

Kautz, L., Jung, G., Du, X., Gabayan, V., Chapman, J., Nasoff, M., Nemeth, E., and Ganz, T. (2015). Erythroferrone contributes to hepcidin suppression and iron overload in a mouse model of beta-thalassemia. Blood *126*, 2031-2037.

Kautz, L., Jung, G., Nemeth, E., and Ganz, T. (2014a). Erythroferrone contributes to recovery from anemia of inflammation. Blood *124*, 2569-2574.

Kautz, L., Jung, G., Valore, E.V., Rivella, S., Nemeth, E., and Ganz, T. (2014b). Identification of erythroferrone as an erythroid regulator of iron metabolism. Nat Genet *46*, 678-684.

Kearney, S.L., Nemeth, E., Neufeld, E.J., Thapa, D., Ganz, T., Weinstein, D.A., and Cunningham, M.J. (2007). Urinary hepcidin in congenital chronic anemias. Pediatr Blood Cancer *48*, 57-63.

Kim, H.S., Neugebauer, J., McKnite, A., Tilak, A., and Christian, J.L. (2019). BMP7 functions predominantly as a heterodimer with BMP2 or BMP4 during mammalian embryogenesis. Elife *8*.

Koch, P.S., Olsavszky, V., Ulbrich, F., Sticht, C., Demory, A., Leibing, T., Henzler, T., Meyer, M., Zierow, J., Schneider, S., et al. (2017). Angiocrine Bmp2 signaling in murine liver controls normal iron homeostasis. Blood *129*, 415-419.

Korchynskyi, O., and ten Dijke, P. (2002). Identification and functional characterization of distinct critically important bone morphogenetic protein-specific response elements in the Id1 promoter. J Biol Chem *277*, 4883-4891.

Little, H.C., Rodriguez, S., Lei, X., Tan, S.Y., Stewart, A.N., Sahagun, A., Sarver, D.C., and Wong, G.W. (2019). Myonectin deletion promotes adipose fat storage and reduces liver steatosis. FASEB J *33*, 8666-8687.

Liu, Q., Davidoff, O., Niss, K., and Haase, V.H. (2012). Hypoxia-inducible factor regulates hepcidin via erythropoietin-induced erythropoiesis. J Clin Invest *122*, 4635-4644.

Luo, G., Hofmann, C., Bronckers, A.L., Sohocki, M., Bradley, A., and Karsenty, G. (1995). BMP-7 is an inducer of nephrogenesis, and is also required for eye development and skeletal patterning. Genes Dev *9*, 2808-2820.

Macotela, Y., Emanuelli, B., Mori, M.A., Gesta, S., Schulz, T.J., Tseng, Y.H., and Kahn, C.R. (2012). Intrinsic differences in adipocyte precursor cells from different white fat depots. Diabetes *61*, 1691-1699.

McCranor, B.J., Langdon, J.M., Prince, O.D., Femnou, L.K., Berger, A.E., Cheadle, C., Civin, C.I., Kim, A., Rivera, S., Ganz, T., et al. (2013). Investigation of the role of interleukin-6 and hepcidin antimicrobial peptide in the development of anemia with age. Haematologica *98*, 1633-1640.

Melchert, J., Henningfeld, K.A., Richts, S., Lingner, T., Jonigk, D., and Pieler, T. (2020). The secreted BMP antagonist ERFE is required for the development of a functional circulatory system in Xenopus. Dev Biol *459*, 138-148.

Mishina, Y., Starbuck, M.W., Gentile, M.A., Fukuda, T., Kasparcova, V., Seedor, J.G., Hanks, M.C., Amling, M., Pinero, G.J., Harada, S., et al. (2004). Bone morphogenetic protein type IA receptor signaling regulates postnatal osteoblast function and bone remodeling. J Biol Chem *279*, 27560-27566.

Mleczko-Sanecka, K., Casanovas, G., Ragab, A., Breitkopf, K., Muller, A., Boutros, M., Dooley, S., Hentze, M.W., and Muckenthaler, M.U. (2010). SMAD7 controls iron metabolism as a potent inhibitor of hepcidin expression. Blood *115*, 2657-2665.

Morrissey, J., Hruska, K., Guo, G., Wang, S., Chen, Q., and Klahr, S. (2002). Bone morphogenetic protein-7 improves renal fibrosis and accelerates the return of renal function. J Am Soc Nephrol *13 Suppl 1*, S14-21.

Murali, D., Yoshikawa, S., Corrigan, R.R., Plas, D.J., Crair, M.C., Oliver, G., Lyons, K.M., Mishina, Y., and Furuta, Y. (2005). Distinct developmental programs require different levels of Bmp signaling during mouse retinal development. Development *132*, 913-923.

Musallam, K.M., and Taher, A.T. (2012). Mechanisms of renal disease in beta-thalassemia. J Am Soc Nephrol *23*, 1299-1302.

Nemeth, E., Tuttle, M.S., Powelson, J., Vaughn, M.B., Donovan, A., Ward, D.M., Ganz, T., and Kaplan, J. (2004). Hepcidin regulates cellular iron efflux by binding to ferroportin and inducing its internalization. Science *306*, 2090-2093.

Ong, D.B., Colley, S.M., Norman, M.R., Kitazawa, S., and Tobias, J.H. (2004). Transcriptional regulation of a BMP-6 promoter by estrogen receptor alpha. J Bone Miner Res *19*, 447-454.

Pak, M., Lopez, M.A., Gabayan, V., Ganz, T., and Rivera, S. (2006). Suppression of hepcidin during anemia requires erythropoietic activity. Blood *108*, 3730-3735.

Papakonstantinou, O., Alexopoulou, E., Economopoulos, N., Benekos, O., Kattamis, A., Kostaridou, S., Ladis, V., Efstathopoulos, E., Gouliamos, A., and Kelekis, N.L. (2009). Assessment of iron distribution between liver, spleen, pancreas, bone marrow, and myocardium by means of R2 relaxometry with MRI in patients with beta-thalassemia major. J Magn Reson Imaging *29*, 853-859.

Peterson, K.R., Fedosyuk, H., Zelenchuk, L., Nakamoto, B., Yannaki, E., Stamatoyannopoulos, G., Ciciotte, S., Peters, L.L., Scott, L.M., and Papayannopoulou, T. (2004). Transgenic Cre expression mice for generation of erythroid-specific gene alterations. Genesis *39*, 1-9.

Ramos, E., Kautz, L., Rodriguez, R., Hansen, M., Gabayan, V., Ginzburg, Y., Roth, M.P., Nemeth, E., and Ganz, T. (2011). Evidence for distinct pathways of hepcidin regulation by acute and chronic iron loading in mice. Hepatology *53*, 1333-1341.

Rodda, C.P., Reid, E.D., Johnson, S., Doery, J., Matthews, R., and Bowden, D.K. (1995). Short stature in homozygous beta-thalassaemia is due to disproportionate truncal shortening. Clin Endocrinol (Oxf) *42*, 587-592.

Songdej, D., Babbs, C., Higgs, D.R., and Consortium, B.I. (2017). An international registry of survivors with Hb Bart's hydrops fetalis syndrome. Blood *129*, 1251-1259.

Suresh, S., Rajvanshi, P.K., and Noguchi, C.T. (2019). The Many Facets of Erythropoietin Physiologic and Metabolic Response. Front Physiol *10*, 1534.

Tsuji, K., Bandyopadhyay, A., Harfe, B.D., Cox, K., Kakar, S., Gerstenfeld, L., Einhorn, T., Tabin, C.J., and Rosen, V. (2006). BMP2 activity, although dispensable for bone formation, is required for the initiation of fracture healing. Nat Genet *38*, 1424-1429.

Tyler, P.A., Madani, G., Chaudhuri, R., Wilson, L.F., and Dick, E.A. (2006). The radiological appearances of thalassaemia. Clin Radiol *61*, 40-52.

Wang, C.Y., Xu, Y., Traeger, L., Dogan, D.Y., Xiao, X., Steinbicker, A.U., and Babitt, J.L. (2020). Erythroferrone lowers hepcidin by sequestering BMP2/6 heterodimer from binding to the BMP type I receptor ALK3. Blood *135*, 453-456.

Yanagita, M., Okuda, T., Endo, S., Tanaka, M., Takahashi, K., Sugiyama, F., Kunita, S., Takahashi, S., Fukatsu, A., Yanagisawa, M., et al. (2006). Uterine sensitization-associated gene-1 (USAG-1), a novel BMP antagonist expressed in the kidney, accelerates tubular injury. J Clin Invest *116*, 70-79.

Yoon, B.S., Ovchinnikov, D.A., Yoshii, I., Mishina, Y., Behringer, R.R., and Lyons, K.M. (2005). Bmpr1a and Bmpr1b have overlapping functions and are essential for chondrogenesis in vivo. Proc Natl Acad Sci U S A *102*, 5062-5067.

Zeisberg, M., Bottiglio, C., Kumar, N., Maeshima, Y., Strutz, F., Muller, G.A., and Kalluri, R. (2003). Bone morphogenic protein-7 inhibits progression of chronic renal fibrosis associated with two genetic mouse models. Am J Physiol Renal Physiol *285*, F1060-1067.

Zhou, S., Turgeman, G., Harris, S.E., Leitman, D.C., Komm, B.S., Bodine, P.V., and Gazit, D. (2003). Estrogens activate bone morphogenetic protein-2 gene transcription in mouse mesenchymal stem cells. Mol Endocrinol *17*, 56-66.
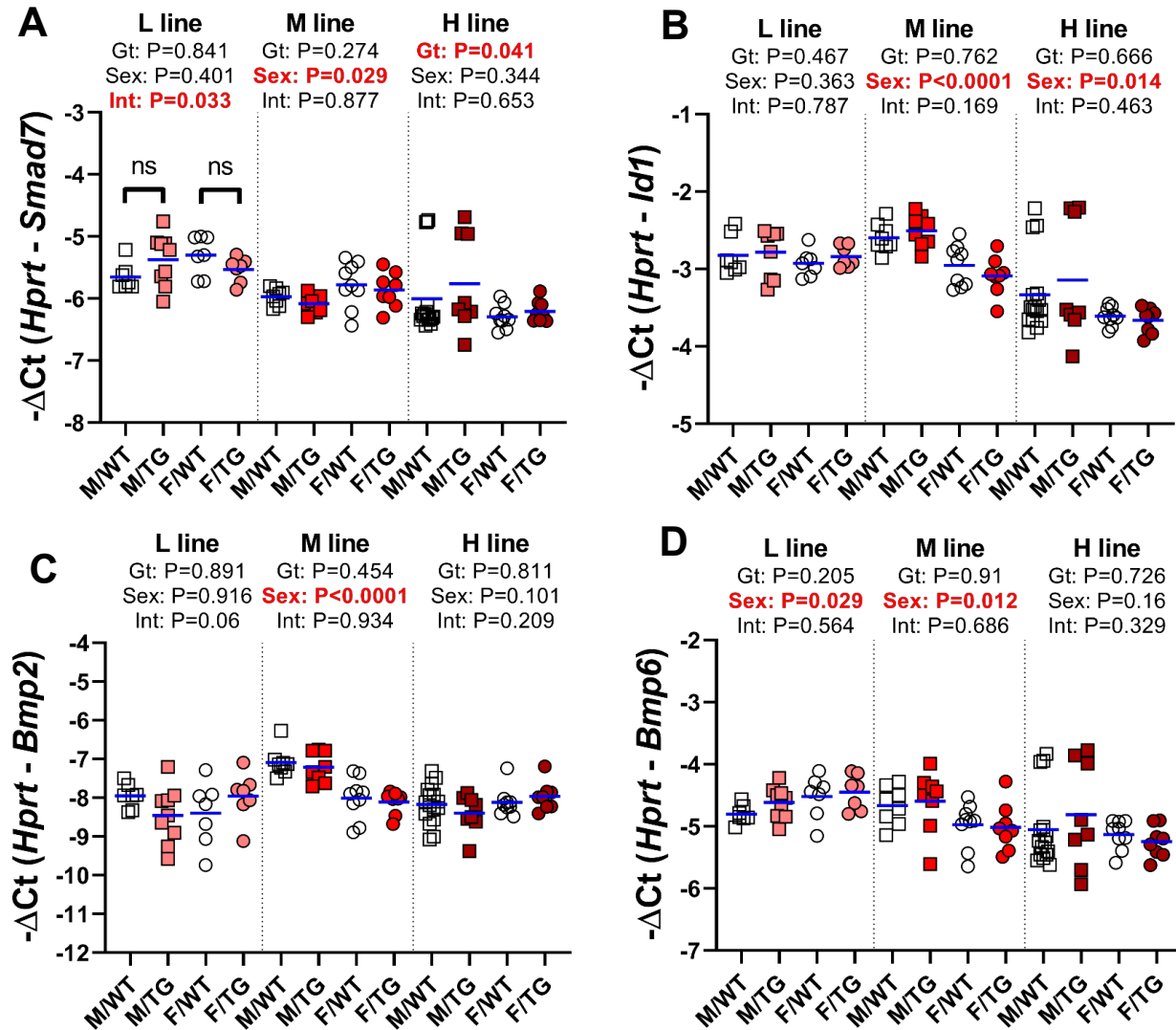
# Supplemental Material



**Figure S1. Effect of *Erfe* overexpression on bone marrow BMP signaling.** Relative mRNA expression of **A)** *Smad7*, **B)** *Id1*, **C)** *Bmp2*, **D)** *Bmp6* in the bone marrow at 6 weeks of age in male (M) and female (F) *Erfe*-overexpressing (TG) mice and wild-type (WT) littermate controls from line-L (white/pink), line-M (white/red), and line-H (white/dark red); group mean is in blue. Groups within each individual line were compared by two-way ANOVA to determine significant effects of genotype and sex on data variation and to identify interactions between these variables (P<0.05 denoted in bold red). In the event of significant interaction between genotype and sex, individual groups were compared by Šidak's multiple comparisons test (NS=P≥0.05, *=P<0.05, **=P<0.01, ***=P<0.001, ****=P<0.0001).
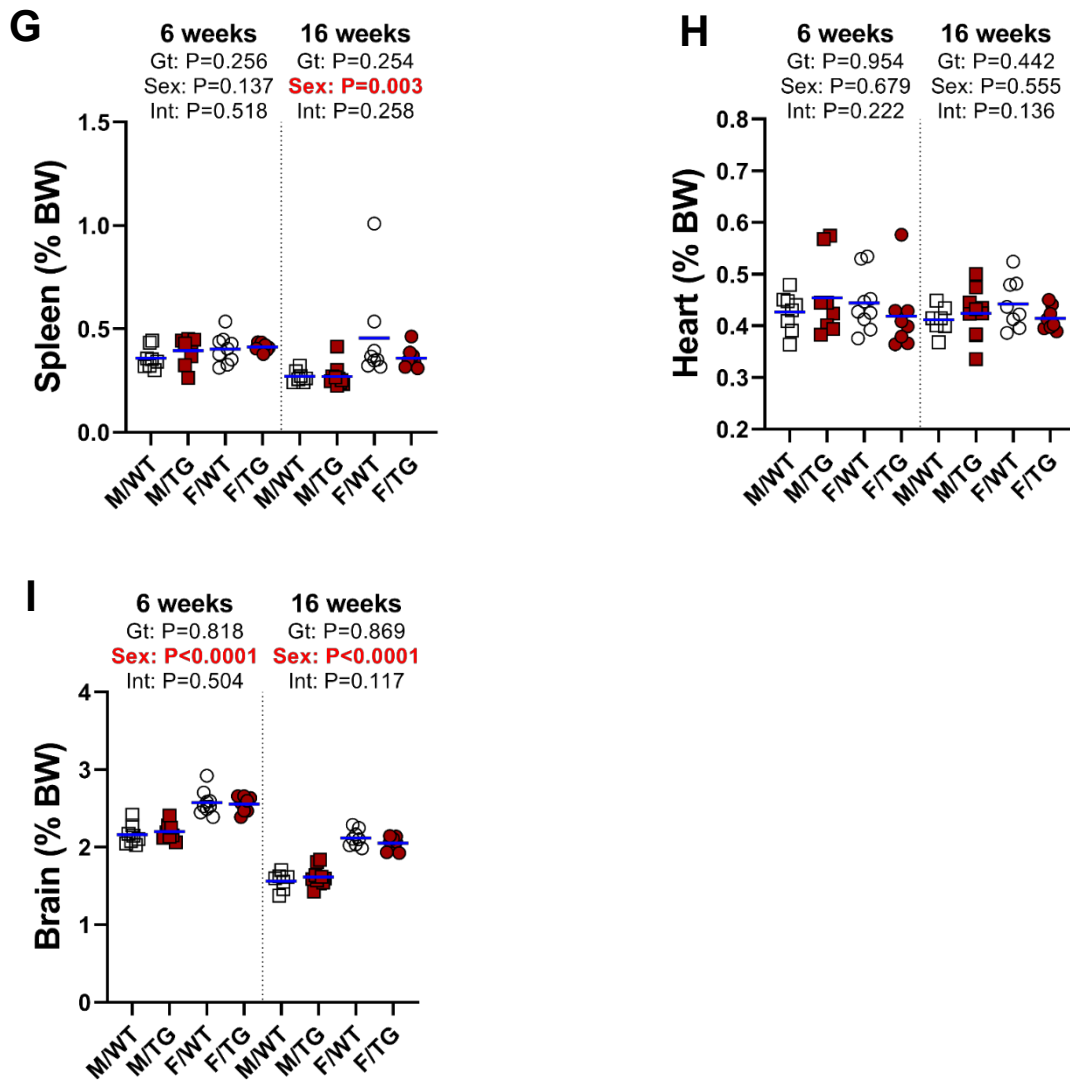
1

(continued)

2
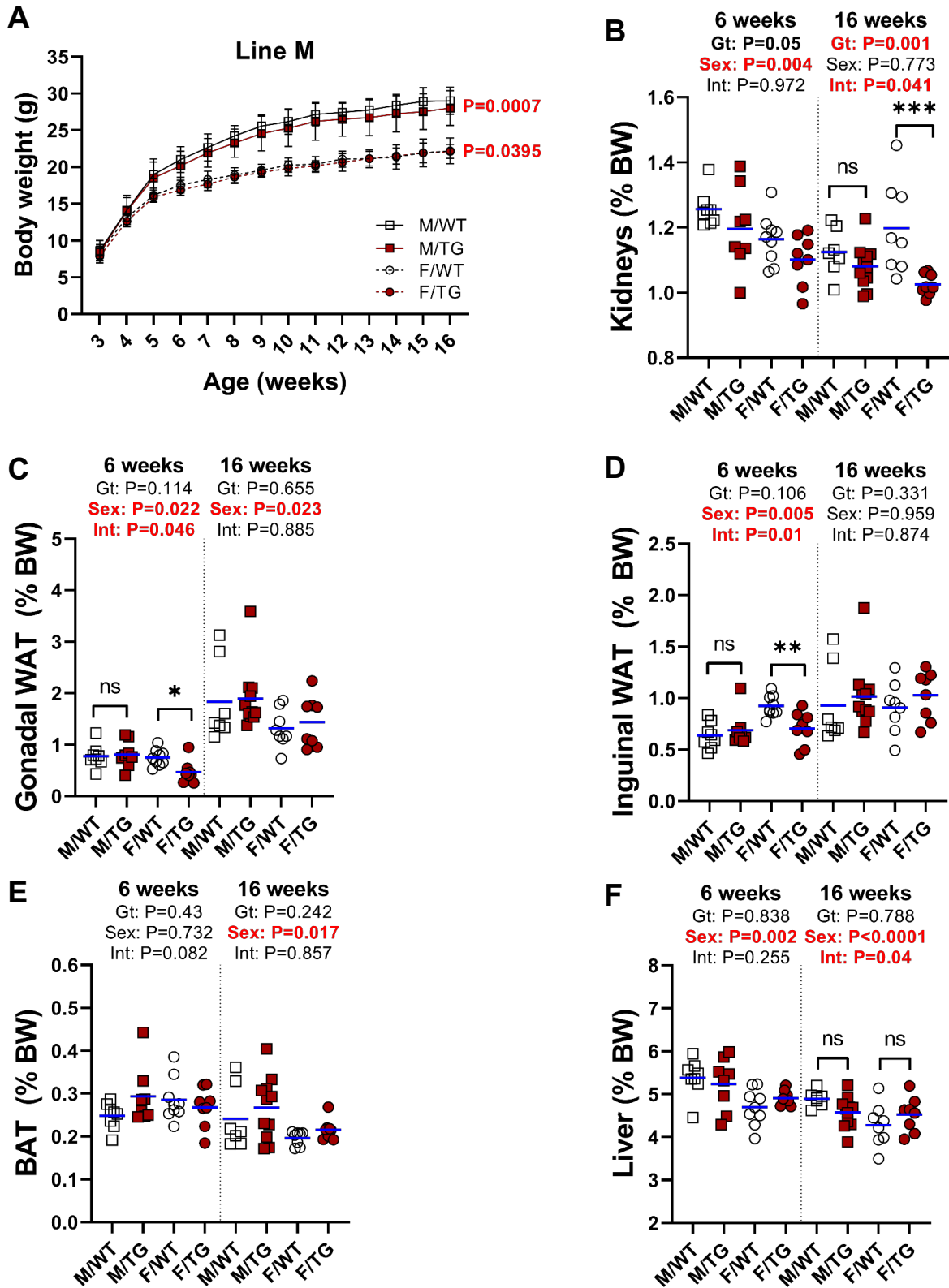
(continued from previous page)



**Figure S2. Growth and tissue mass in line-M mice. A)** Growth curves of line-M mice from ages 3 to 16 weeks of age. Statistical significance of the effect of genotype on data variation between body weights of sex-matched wild type (WT) and transgenic (TG) mice determined by 2-way ANOVA are displayed to the right of their respective curves. Statistically significant differences (P<0.05) between sex-matched WT and TG body weights at individual time points, determined by Student's $t$-test, are indicated by asterisks (*) above or below curves for males and females, respectively. Mass of **B)** kidneys, **C)** gonadal white adipose tissue (WAT) pads, **D)** inguinal white adipose tissue (WAT) fat pads **E)** interscapular brown adipose tissue (BAT), **F)** liver, **G)** spleen, **H)** heart, and **I)** brain at 6 and 16 weeks of age relative to total body mass; group mean is in blue. Groups at each age were compared by two-way ANOVA to determine significant effects (P<0.05) of genotype and sex on data variation and to identify interactions between these variables. In the event of significant interaction between genotype and sex, individual groups were compared by Šidak's multiple comparisons test (NS=P≥0.05, *=P<0.05, **=P<0.01, ***=P<0.001).
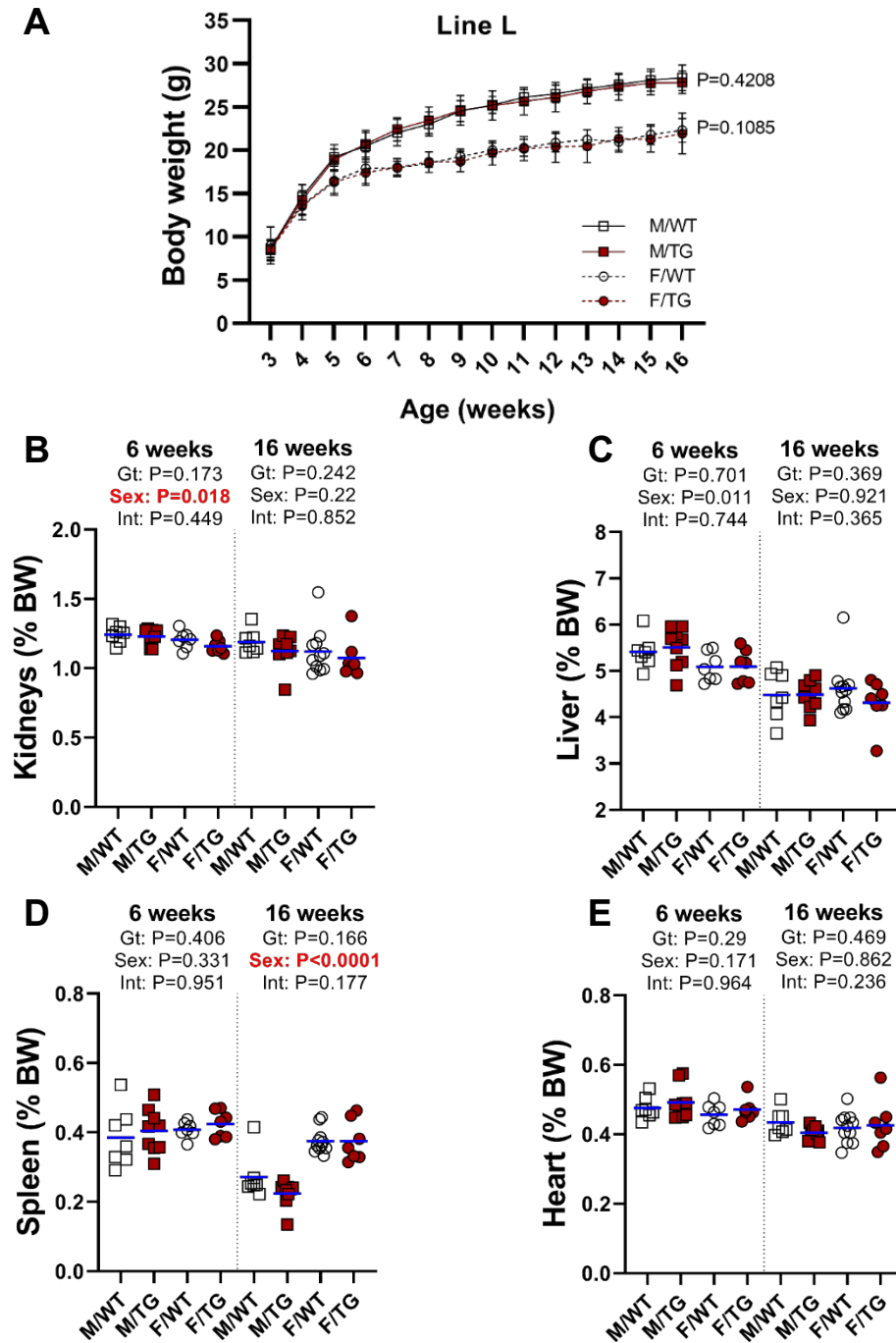
**Figure S3. Growth and tissue mass in line-L mice. A)** Growth curves of line-L mice from ages 3 to 16 weeks. Statistical significance of the effect of genotype on data variation between body weights of sex-matched wild type (WT) and transgenic (TG) mice determined by 2-way ANOVA are displayed to the right of their respective curves. Statistically significant differences (P<0.05) between sex-matched WT and TG body weights at individual time points, determined by Student's T-test, are indicated by asterisks (*) above or below curves for males and females, respectively. Mass of **B**) kidneys, **C**) liver, **D**) spleen, and **E**) heart at 6 and 16 weeks of age relative to total body mass. Groups at each age were compared by two-way ANOVA to determine significant effects (P<0.05) of genotype and sex on data variation and to identify interactions between these variables.
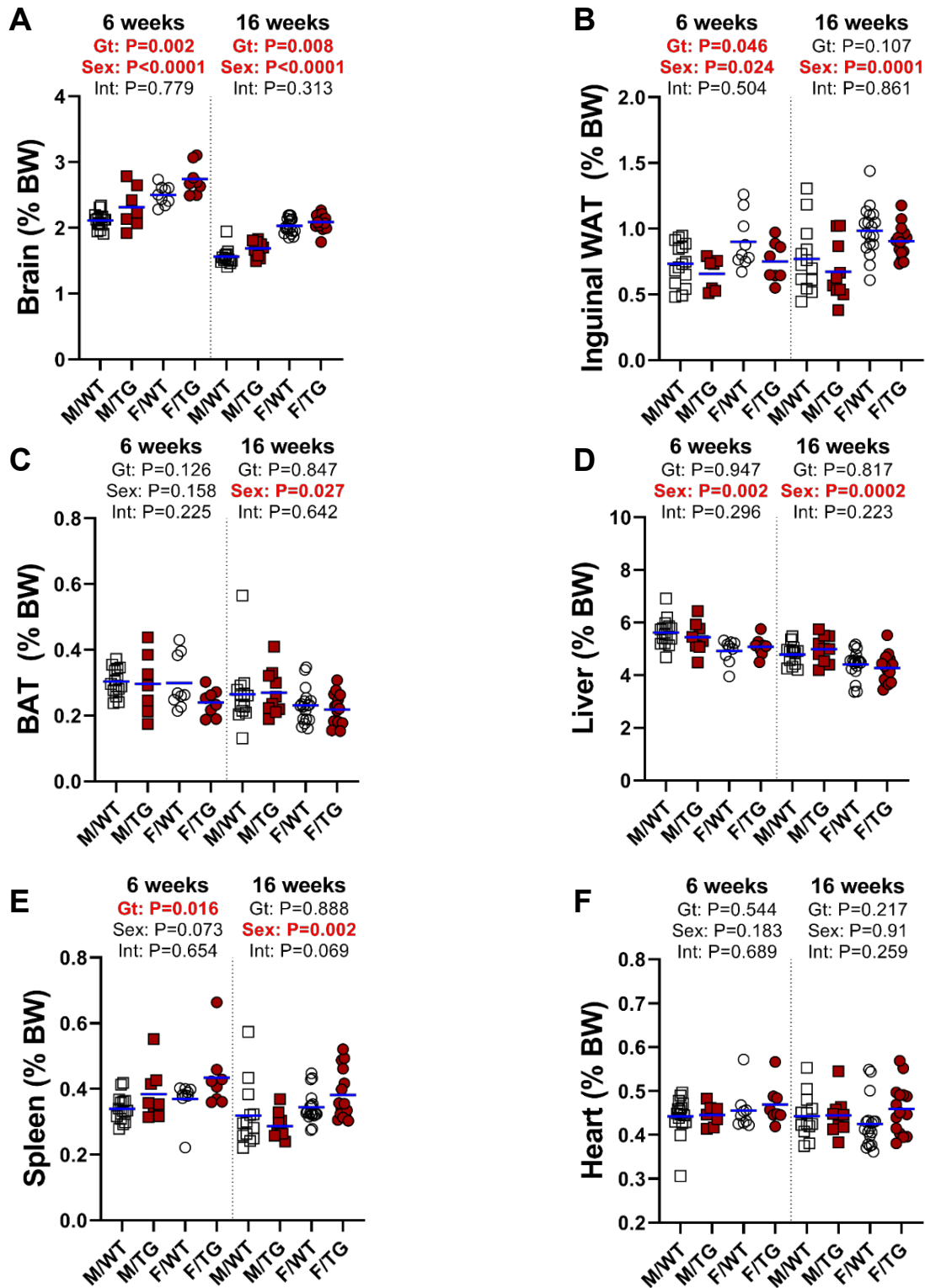
4

**Figure S4. Mass of various tissues from line-H mice.** Mass of **A**) brain, **B**) inguinal white adipose tissue (WAT) fat pads, **C**) interscapular brown adipose tissue (BAT), **D**) liver, **E**) spleen, and **F**) heart at 6 and 16 weeks of age relative to total body mass. Groups at each age were compared by two-way ANOVA to determine significant effects (P<0.05) of genotype and sex on data variation and to identify interactions between these variables.
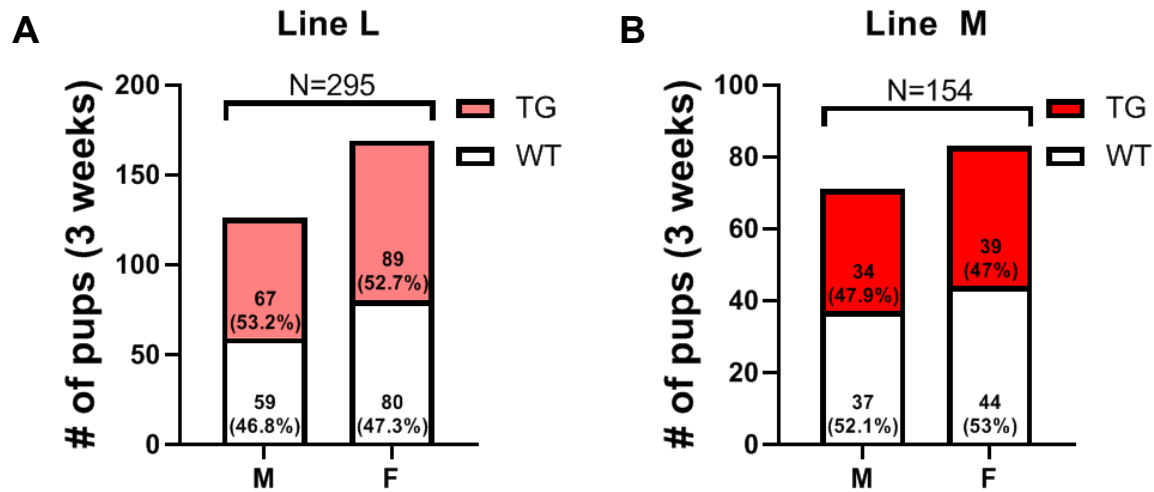
**Figure S5. Normal postnatal survival of line-L and line-M transgenic mice.** Number and within-sex percentage of wild-type (WT) and transgenic (TG) mice, grouped by sex, from **A**) line-L and **B**) line-M mice surviving at 3 weeks of age. Differences from expected proportions were not statistically significant by binomial testing at P<0.05.
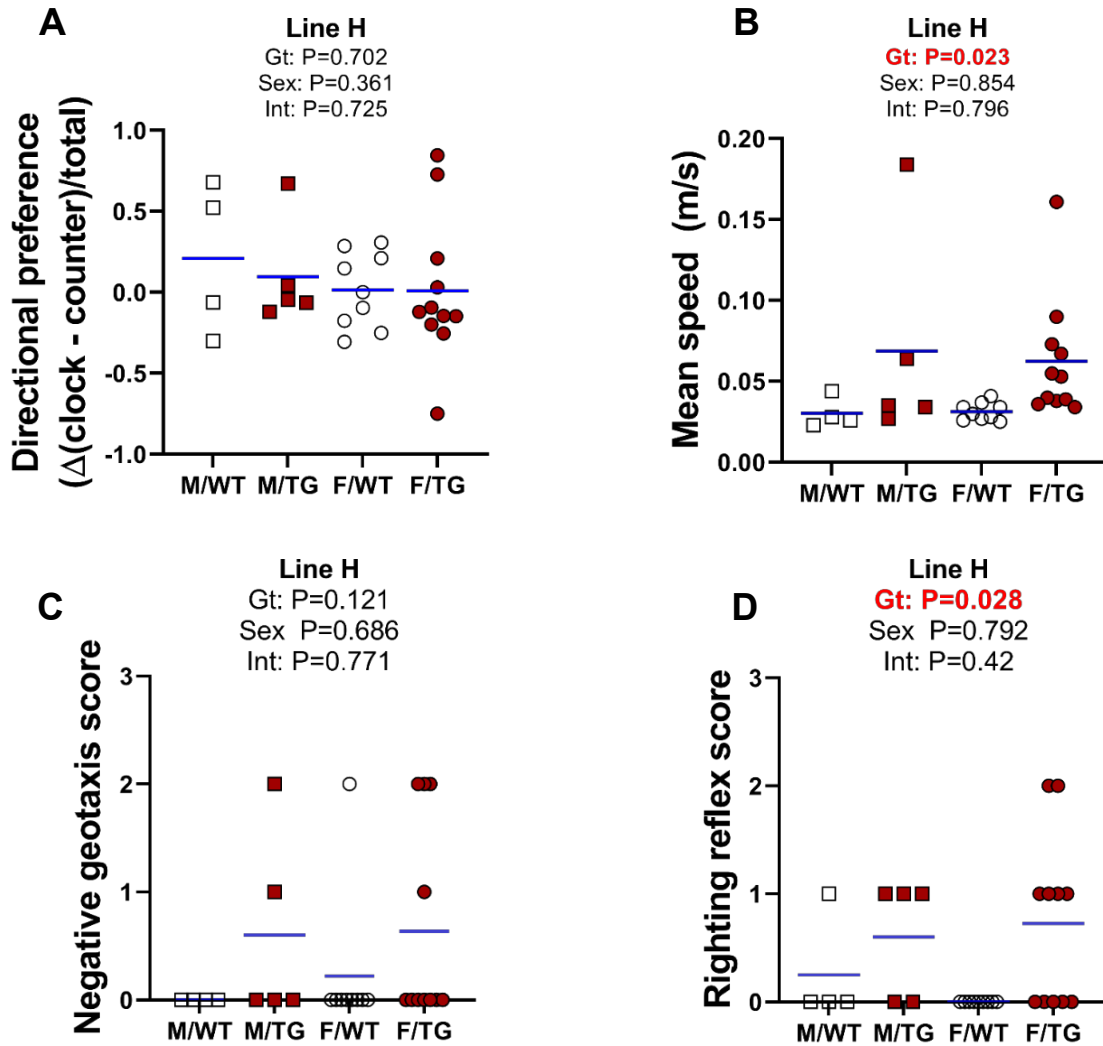
**Figure S6. Behavior testing in line-H mice.** Quantification of **A**) rotation direction preference during open-field testing, **B**) Mean speed of mice during open-field testing, **C**) negative geotaxis and **D**) righting-reflex test performance. Groups were compared by two-way ANOVA to determine significant effects (P<0.05) of genotype and sex on data variation and to identify interactions between these variables.

| | F:5'---3' | R:5'---3' |
|---|---|---|
| mHprt | CTGGTTAAGCAGTACAGCCCCAA | CAGGAGGTCCTTTTCACCAGC |
| mErfe | ATGGGGCTGGAGAACAGC | TGGCATTGTCCAAGAAGACA |
| mHamp | TTGCGATACCAATGCAGAAGA | GATGTGGCTCTAGGCTATGTT |
| mId1 | ACCCTGAACGGCGAGATCA | TCGTCGGCTGGAACACATG |
| mSmad7 | TTGCCTCGGACAGCTCAATTC | CGCACTTTCTGTACCAGCTGA |
| mBmp2 | GATCTGTACCGCAGGCACTC | CCGTTTTCCCACTCATCTCT |
| mBmp6 | ATGGCAGGACTGGATCATTGC | CCATCACAGTAGTTGGCAGCG |

**Table S1. Primer sequences used for qRT-PCR**

| | Units | abbreviation | WT (mean ± SD) | TG (mean ± SD) | P value |
|---|---|---|---|---|---|
| Tissue area | mm$^2$ | T.Ar | 2.871 ± 0.038 | 2.86 ± 0.064 | 0.718 |
| Bone volume/tissue volume | % | BV/TV | 11.39 ± 4.307 | 12.9 ± 0.808 | 0.434 |
| Osteoid volume/bone volume | % | OV/BV | 0.611 ± 0.0514 | 0.704 ± 0.523 | 0.748 |
| Osteoid surface/bone surface | % | OS/BS | 6.349 ± 3.079 | 5.821 ± 3.285 | 0.765 |
| osteoblast surface/bone surface | % | Ob.S/BS | 21.97 ± 5.136 | 20.06 ± 5.709 | 0.53 |
| Osteoclast surface/bone surface | % | Oc.S/BS | 4.035 ± 1.009 | 4.179 ± 0.875 | 0.78 |
| Eroded surface/bone surface | % | ES/BS | 7.652 ± 1.846 | 7.986 ± 1.763 | 0.736 |
| Trabecular thickness | μm | Tb.Th | 29.37 ± 3.29 | 30.44 ± 1.718 | 0.444 |
| Osteoid thickness | μm | O.Th | 1.223 ± 0.429 | 1.653 ± 0.386 | 0.073 |
| Osteoblast #/bone perimeter | /mm | N.Ob/B.Pm | 19.82 ± 4.51 | 18.28 ± 5.14 | 0.573 |
| Osteoclast #/eroded perimeter | /mm | N.Oc/E.Pm | 31.45 ± 2.682 | 30.8 ± 2.68 | 0.658 |
| Trabecular separation | μm | Tb.Sp | 251.8 ± 81.324 | 206.4 ± 18.806 | 0.233 |
| Trabecular # | /mm | Tb.N | 3.824 ± 1.145 | 4.248 ± 0.343 | 0.415 |

**Table S2. Bone histomorphometry analysis.** Femurs from 6-week old female wild-type (WT, n=6) and transgenic (TG, n=8) littermate mice were compared using Student t-test.